Review

Recent progressive use of advanced atomic force microscopy in polymer science: A review

Phuong Nguyen-Tri [1*], Payman Ghassemi[1], Pascal Carriere[2], Aymen Amine Assadi[3], Dinh Duc Nguyen[4]

1. Département de chimie, biochimie et physique, Université du Québec à Trois-Rivières (UQTR), Québec, G8Z 4M3, Canada. Email : Phuong.Nguyen-Tri@uqtr.ca; payman.ghassemi3@gmail.com
2. Laboratoire MAPIEM (EA 4323), Matériaux Polymères Interfaces Environnement Marin, Université de Toulon, Toulon, France. Email : pascal.carriere@univ-tln.fr
3. Univ Rennes, ENSCR- Institut des Sciences Chimiques de Rennes (ISCR) - UMR CNRS 6226, France. aymen.assadi@ensc-rennes.fr
4. Department of Environmental Energy Engineering, Kyonggi University, Suwon, Republic of Korea, email: nguyensyduc@gmail.com

* Correspondence: Phuong.nguyen-tri@uqtr.ca; Tel.: +819-376 5011 (ext. 4505)

Abstract: Atomic force microscopy (AFM) has been extensively used for the nanoscale characterization of polymeric materials. The coupling of AFM with infrared spectroscope (AFM-IR) provides another advantage to the chemical analyses and thus helps to shed light upon the study of polymers. In this perspective paper, we review recent progress in the use of AFM-IR in polymer science. We describe first the principle of AFM-IR and the recent improvements to enhance its resolution. We discuss then the last progress in the use of AFM-IR as a super-resolution correlated scanned-probe IR spectroscopy for chemical characterization of polymer materials dealing with polymer composites, polymer blends, multilayers and biopolymers. To highlight the advantages of AFM-IR, we report here several results in studying crystallization of both miscible and immiscible blends as well as polymer aging. Then, we demonstrate how this novel technique can be used to determine phase separation, spherulitic structure and crystallization mechanisms at nanoscales, which have never been achieved before. The review also discusses future trends in the use of AFM-IR in polymer materials, especially in polymer thin film investigation.

Keywords: AFM-IR, polymers, polymer composites, blends, polymer aging, nanoscale characterization, nanoscale characterization.

1. Introduction

FT-IR is one of the most powerful spectroscopic techniques for the characterization and identification of numerous materials, especially for the polymers, biomaterials and life science [1-5]. However, the main drawback of FTIR method relates to its low spatial resolution of three times the wavelength of the IR radiations (under 20 μm). The addition of several special devices like attenuated total reflection crystals in an IR spectroscopy (ATR-FTIR) allows to analysis with penetration depth into the sample between 0.5 and 2 μm [6]. Nevertheless, ATR-FTIR can be only achieved on a spatial resolution approaching the wavelength with a sample thickness of 3-10 μm [6-11]. In contrast, the atomic force microscope (AFM) [12] is considered a useful tool for the nanoscale measurement in polymer science and engineering [13-15], especially for studying complex [16-25]. Various new discoveries have been reported in the literature with this nanoscale imaging technique [26-34] structures and polymer crystallization. However, the AFM lacks the robust ability to chemically

characterize materials. Although there have been some encouraging attempts to combine AFM with several optical techniques, until recently they have been limited in wavelength range or spatial resolution. The coupling of AFM with infrared and Raman spectroscopic with nanometer-scale resolution [35-44], including tip-enhanced Raman spectroscopy (TERS) [45, 46] infrared scattering-type scanning near-field optical microscopy (IR s-SNOM)[47],thermocouple (nano-TA)[48-51] atomic force microscopy-infrared spectroscopy (AFM-IR)[52-55], and photo-induced force microscopy (PiFM)[56], atomic force microscopy nuclear-magnetic resonance (AFM-NMR)[57], atomic force microscopy nuclear- rheometer (Nano-rheology)[58, 59] were recently developed to overcome these drawbacks. Details about these technologies can be found in previous review articles [60-63]. AFM-IR can measure and map local chemical composition below the diffraction limit, as well as nanoscale topographic, mechanical, and thermal analysis [60]. This method has been considered one of the most important recent developments in sub-micrometer spectroscopies and chemical imaging. The use of this technique has shed light on many assumptions and provided new mechanisms in investigation of polymer materials [64, 65]. Nowadays, AFM-IR has been used to analyze various materials including polymer blends [66, 67], polymer composites [68-71], multilayer films [72], polymer thin films [55, 73] life sciences [36, 38, 54, 74, 75] as well as pharmaceutical blend systems[60]. Additionally, by tuning the source to a fixed wavelength and measuring the deflection as a function of position across the sample, it can obtain AFM-IR images showing the distribution of chemical species of interest. Mechanical and thermal properties of the sample can also be obtained by AFM-IR with suitable devices [76]. The AFM-IR can be quickly provided both a nanoscale AFM image and high-resolution chemical spectra at selected regions on the sample and thus helps to identify or quantitative analyses of the complex systems. Although there have been several review articles on the use of AFM and AFM-IR [60-63] in material science, it lacks an overview of the usefulness of this technique to polymer science. Moreover, the information of the recent applications of AFM-IR in polymer crystallization is lacking. The goal of this review is to provide to readers the latest progress in the use of AFM and AFM-IR in polymers blends, polymer composites, multilayers and especially on polymer aging as well as on crystallization studies.

2. The principle of AFM

Atomic force microscopy (AFM) is a tool for the study of phenomena at the nanoscale, which includes quantitative single molecule studies[29].AFM is an unparalleled tool for observing temporal changes introduction in polymer morphology. The development of devices that operate at elevated temperature has enabled the direct observation of polymer crystallization and melting, as well as structural changes occurring during the annealing of thin, metastable lamellar crystals[77]. As an important tool, atomic force microscopy (AFM) was commonly used in the field of polymer crystallization. Generally, the effect of the AFM tip throughout the scan should be diminished in order to truly reflect the crystal morphology and crystallization mechanism[78]. It is a high-resolution technology, regularly with the resolution of sub 10 nm features[79, 80], and due to enable the fundamental length scale of the polymer lamellar crystal, its thickness, to be perceived.

AFM does not require sample staining or metal coating, so it is straightforward to prepare the specimen. In many cases, it is also non-destructive. It makes images to be captured whereas a process

Peer-reviewed version available at Polymers 2020, 12, 1142; doi:10.3390/polym12051142

such as melting or crystal growth occurs, providing lamellar or sub-lamellar resolution time-resolved data [81-84].

It is a final feature that provides many of AFM's most interesting opportunities to study polymer crystallization, as it is now possible to observe crystal melting, crystal growth and lamellar-scale reorganizations within crystals, seeing how structure evolve and local conditions affect kinetics[84].

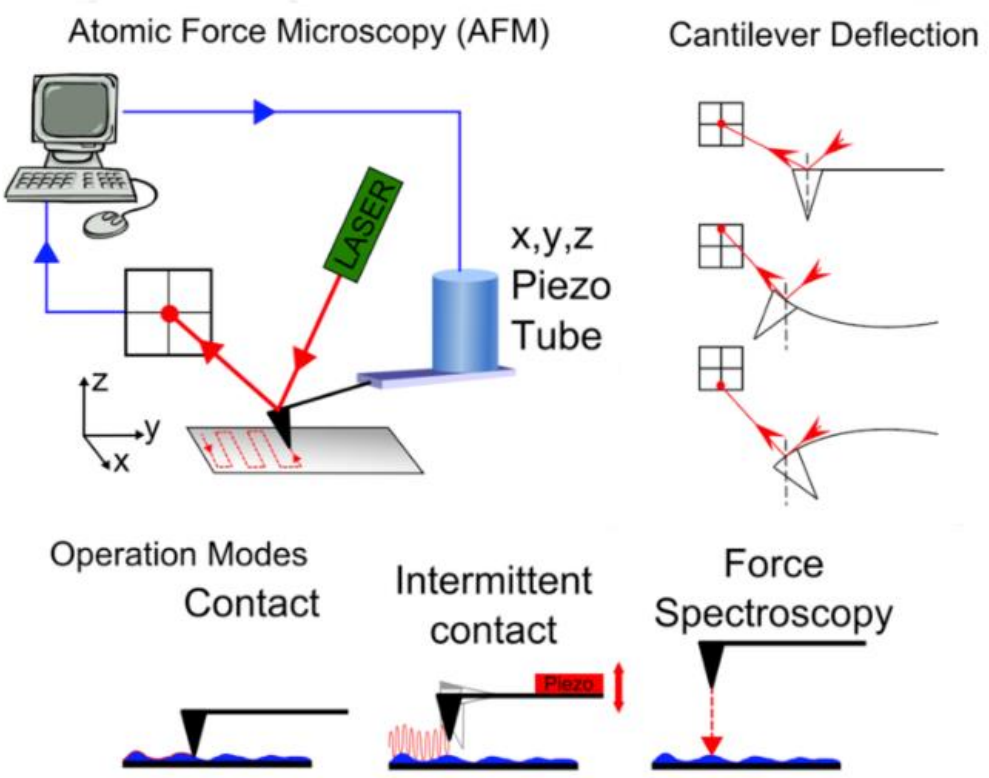

Figure 1. A schematic of an Atomic Force Microscopy (AFM) set-up and Cantilever Deflection (Adopted from https://covalentmetrology.com/afm/).

A graphic of an AFM set-up is displayed in Figure 1. The main element is sensor, a pyramidal tip attached to a 100-400 µm long cantilever, which is in contact with the sample surface. Cantilever and tip are often made of silicon or silicon nitride, because these materials allow relatively low-cost mass production using semi-conductor technology. The geometry of the apex of the tip is representing one of the key parameters determining the resolution. With a tip that ends in a single atom, the highest resolutions can be reached. The cantilever is a system comparable to a contact profilometry, with the three-dimensional displacement of the AFM tip relative to the pattern being received with the aid of piezoelectric crystals. This set-up allows for placing of the AFM tip with an accuracy of approx. 1 nm in x-, y- and z-direction. When the AFM tip is engaging a surface, the cantilever is bending due to repulsive forces between tip and sample. This deflection, proportional to the pressure either being applied to the specimen, is used to represent a topography of the surface directly or as an input for the feedback loop controlling the AFM's z-position [85]. There are several different techniques for quantifying this deflection [86]. However, the most common use of an optical sensor is a laser beam that is reflected from the cantilever backside to a position-sensitive light

Peer-reviewed version available at Polymers 2020, 12, 1142; doi:10.3390/polym12051142

detector. Because the laser place on the detector varies in accordance with the degree of bending of the cantilever of the AFM, the latter can be measured accordingly [87].

2.1. AFM Scanning/Operation Modes

AFM can be operated under various modes, the choice of suitable operating mode depends on the desired information and types of AFM image. In summary, there are 3 main operation modes of AFM, they are contact mode, non-contact mode and tapping mode. This classification of the AFM operation modes is based on interactions between tip and surface (Figure 2 & Table 1). More specifically, AFM works in "contact mode" in the presence of constantly repulsive forces or in "non-contact mode" being attractive forces onto the tip. Lastly, AFM may work in tapping mode in the presence of both attractive and repulsive force [88]. For all the operation modes, the images may be reconstructed by recording all interatomic interactions occurring at the end of the tip during the cantilever scanning onto the sample surface [89].

- Static Modes: Contact mode

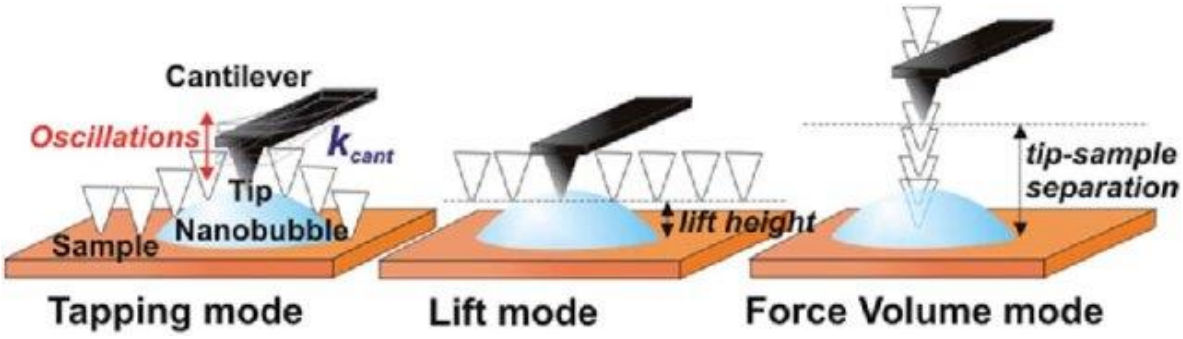

Fig.2. Scanning modes of AFM, adopted from https://pubs.rsc.org/en/content/articlehtml/2014/sm/c4sm01024h

Table 1. Summary of AFM modes of operation (scanning).

(Adapted from Marica M et al, Functional Biomaterials. 2017, 8, 7).

AFM Modes of Operation	Working Principle	Advantage	Disadvantage
Contact Mode	•Physical contact between the tip and the surface	• High scan speeds •High resolution	•Damage to soft sample •Later forces may produce image artefacts
Non-contact Mode	•No contact between the tip and the sample	•Low resolution •No damage to sample	•Slower scan speed if compared with both contact and tapping mode
Tapping Mode	•Intermittent and short contact between the sample and the tip	•High resolution Minimal damage to sample	•Slower scan speed if compared with contact mode

Peer-reviewed version available at Polymers 2020, 12, 1142; doi:10.3390/polym12051142

2.2. Contact mode AFM

Contact is mostly named a static mode, while the other authors prefer to refer to the modes by their detection mechanisms[90]. Tapping mode would then be called Amplitude Modulation AFM (AM-AFM).The contact operational mode is the most suitable for flat and rigid surfaces such as crystal, hard polymers and tissue, enabling the highest resolution level. In this mode, it is possible to capture image artifacts associated with a not-flat surface or to a mechanical drift derived from the scanner motion. These artifacts can prevail the topography image over the real morphological features. To intercept these artefacts and to measure how well the desired deflection set point is maintained constant by the feedback system, the error mode can be used[88].

2.3. Noncontact mode

In non-contact mode, the oscillating probe is generally influenced by the close surface, so producing a frequency shift in the resonant frequency, due to Van der Waals attractive forces. Hence, the signals recorded in non-contact mode are related to the variation between cantilever resonance frequency and free oscillation of the system, giving a preliminary estimation of atomic tip-sample interaction forces intensities [85].

Tapping and noncontact are called dynamic modes, as the cantilever is oscillated in tapping and noncontact modes. Typically, this is done by adding an extra piezoelectric element that oscillates up and down at somewhere between 5-400 kHz to the cantilever holder. Noncontact AFM, unlike the other AFM techniques can obtain true atomic resolution images [90].

2.4. Tapping mode AFM

Lastly, in the case of tapping or intermittent contact AFM (IC-AFM), probe excitation externally occurs, and the amplitude and cantilever phase may be monitored in the proximity of the resonance frequency. With respect to the other operation modes, tapping mode has been employed successfully for the topographic characterization of cell-loaded surfaces, due to the application of lower forces and high-resolution imaging [89].

The main difference between tapping mode and noncontact mode is in tapping mode; the tip of the probe actually touches the sample and moves completely away from the sample in each oscillation cycle. In NC-AFM, the cantilever stays close to the sample all the times and has a much smaller oscillation amplitude. NC-AFM (noncontact AFM) is more sensitive to small oscillations of the cantilever, so may be operated in close contact (almost touching) [90].

Noncontact AFM, unlike the other AFM techniques can obtain true atomic resolution images[89]. AM-AFM is typically used for tapping mode - where the tip actually taps the sample during each oscillation. This is often the most stable mode to use in air, and so is currently more commonly used than either noncontact or contact modes for most applications. The main difference between tapping mode and noncontact mode is that in tapping mode, the tip of the probe actually touches the sample, and moves completely away from the sample in each oscillation cycle. In NC-AFM, the cantilever stays close to the sample all the times, and has a much smaller oscillation amplitude. NC-AFM (noncontact AFM) is more sensitive to small oscillations of the cantilever, so may be operated in close contact (almost touching)[90].

Peer-reviewed version available at Polymers 2020, 12, 1142; doi:10.3390/polym12051142

AM-AFM is typically used for tapping mode - where the tip actually taps the sample during each oscillation. This is often the most stable mode to use in air, and so is currently more commonly used than either noncontact or contact modes for most applications. The main difference between tapping mode and noncontact mode is that in tapping mode, the tip of the probe actually touches the sample, and moves completely away from the sample in each oscillation cycle. In NC-AFM, the cantilever stays close to the sample all the times, and has a much smaller oscillation amplitude. NC-AFM (noncontact AFM) is more sensitive to small oscillations of the cantilever, so may be operated in close contact (almost touching).AM-AFM is typically used for tapping mode - where the tip actually taps the sample during each oscillation. This is often the most stable mode to use in air, and so is currently more commonly used than either noncontact or contact modes for most applications[90].

2.5 Phase imaging

The contrast of an atomic force micrograph generally depends on the mechanical properties of the surface and the probe, for instance, the adhesiveness and elasticity. To produce a sharp image of the surface topography, the sample material has to be relatively rigid compared to the probe. As the material becomes softer, the image obtained will become more influenced by the elastic properties of the surface. In extreme cases, the tip-surface interaction can cause damage or displacement of the sample[34].

Phase imaging, a method closely associated with IC-AFM, enables surface properties to be observed beyond pure topography. Once scanning in IC-AFM, the damping of the oscillation outcomes in a loss of oscillation energy occurred in the cantilever due to energy transfer to the sample. This results in a phase change as well as the lower amplitude of the cantilever oscillation. Since this phase change is a feature of the sample material's energy absorbency, it is idiosyncratic for rigid or soft materials or, more generally, low and high-energy absorbency materials(see Figure 3)[91].

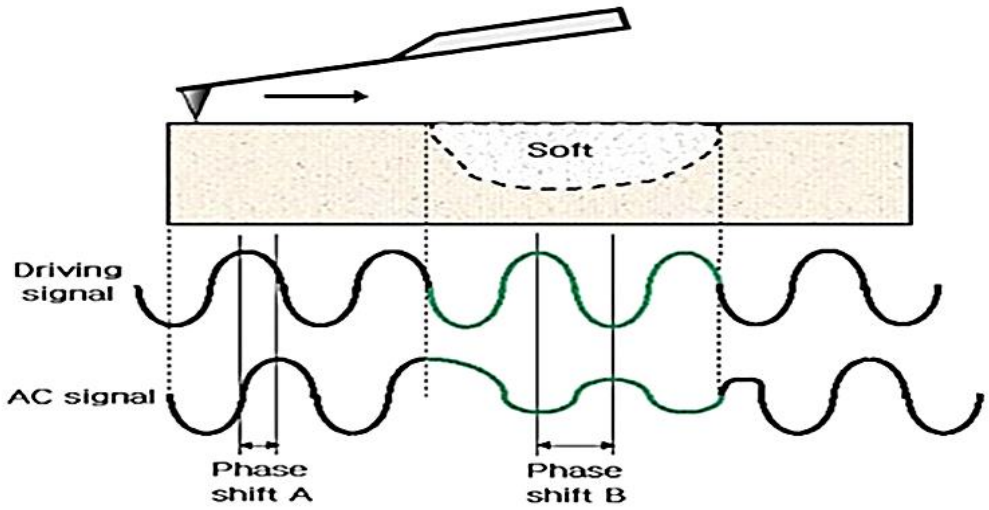

Figure 3. The phase lag changes depending on the mechanical properties of the sample surface, adopted from: https://parksystems.com/park-spm-modes/91-standard-imaging-mode/221-phase-imaging-phase-detection-microscopy-pdm.

Peer-reviewed version available at Polymers 2020, 12, 1142; doi:10.3390/polym12051142

It results in a phase shift of the cantilever oscillation as well as the lower amplitude. As this phase shift is a function of energy absorbency of the sample material, it is idiosyncratic for stiff or soft materials[92], or more precisely, materials with high and low energy absorbency[91]. This allows analyzing the distribution of different materials or phases within the sample, for example, phase separation within lipids[93] or drug distribution within nanoparticles[94].

2.6. Force spectroscopy

AFM also can be used to quantify forces between the tip and the surface of the sample, thereby producing curves of force-distance[95].A sort of forces can be detected. These consist of Coulomb forces, van der Waals forces, electrostatic forces or particular forces between ligand-receptor pairs [96-100]. As mentioned above, AFM's theory is based on determining the forces between the tip of the AFM and the surface of the sample. Therefore, this force purpose can not only be used in a response loop for imaging, but also as an pointer for the power of interaction between sample and tip. The advantage of Atomic Force Spectroscopy (AFS) over the other techniques such as the stylus profile meter is the probe's high lateral positioning, enabling the sample's behavior to be observed at nano-scale resolution and high force sensitivity, enabling forces to be recorded down to the pN range[101].

2.7 Cantilever-tip systems

A key factor for high-resolution imaging is the AFM tip, particularly, its geometry, radius and chemical composition. The AFM tip, in particular its structure, radius and chemical composition, is a key factor for high-resolution imaging. The key limiting factor with respect to an AFM's overall resolution is the tip apex radius. Highlights in the tip's size range are distortedly and extended, highlights that are smaller may not be apparent at all. [102].

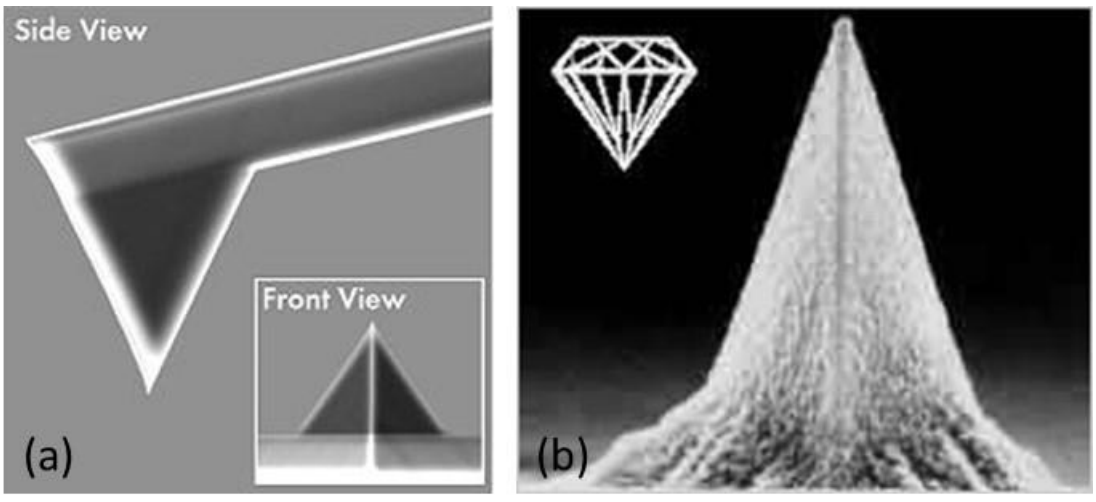

Figure 4. a) AFM Si3N4 tip with Cantilever and d) diamond coated AFM tip, adapted from https://www.nanoandmore.com/AFM-Probe-ARROW-CONTR

For very high (i.e., atomic) resolution, special probes so-called 'supertips' are commercially available. These are also well suited for lateral force measurements or point force measurements (Figure 4a). AFM tips are typically fabricated from materials like silicon or silicon nitride. However, diamond, carbon or single crystals of minerals have been employed for select special applications

Peer-reviewed version available at Polymers 2020, 12, 1142; doi:10.3390/polym12051142

(Figure 4b). Microfabrication etching technique is the most commonly used method for preparing such samples. The cantilever / sample systems are etched using this method from oxidized silicon wafers using photographic masks to describe the cantilever's form. This leads to tips with a radius below 30 nm. Super tips can be generated at the end of pyramidal Si3N4 tips through the regulated growing of carbon filaments [103]. The tips developed by these techniques will be further modified surface yielding well-defined sensor systems at the nano-resolution to characterize the mechanical, elastic and chemical properties of samples. For example, nano-sensors can be produced by covalent binding of molecules such as lipids, DNA, proteins to the surface of the sample based on a wide range of chemical reactions [104].

3. AFM-IR

3.1 The principle of AFM-IR

The principle of AFM-IR[52] is to couple the AFM in contact mode (or taping mode) with a pulsed tunable laser is shown in Figure 5. In the first-generation AFM-IR, a sample is irradiated near field infrared radiations or laser through an infrared-transparent prism (ZnSe). When the laser wavelength is tuned on the absorption bands of the sample, it generates a photo-thermal temperature rise in the absorbing regions of the sample and then, causes a rapid thermal expansion pulsed under the AFM tip (very short, about several tens of microseconds) and creates an exciting resonant oscillation of the AFM cantilever. Therefore, each time, the pulsed light is absorbed and heats the sample; the cantilever oscillates at its resonance frequency leading to absorption spectra that are to those obtained by traditional FTIR spectroscopy. Each absorption peak corresponds to excitation of a specific molecular resonance and the pattern of peaks, i.e. the absorption spectrum acts as a unique chemical fingerprint of the nanoscale region of the sample as shown in Figure 5.

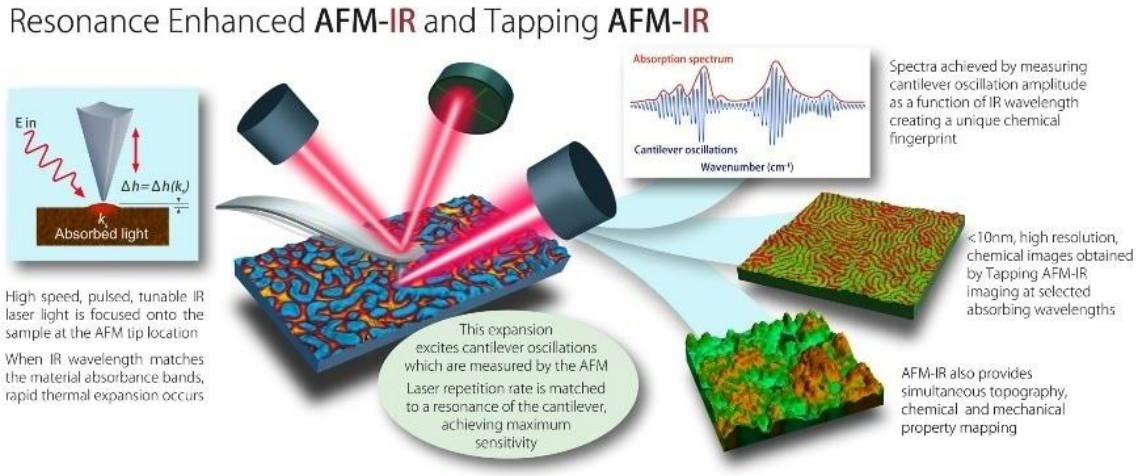

Figure 5. Scheme depicting the principle of the AFM-IR technique. The sample is deposited on a ZnSe-prism and illuminated by a tunable, pulsed IR-laser (total internal reflection geometry). The probe consists of a standard AFM-lever and detection system (Adopted from: https://www.azonano.com/article.aspx?ArticleID=4509).

Although, the AFM allows analyzing samples with a spatial resolution order of 50-100 nm, its resolution is mainly determined by the thickness of samples. Because the thermal expansion is three-dimensional and thus to achieve the spatial resolution of a few hundred nanometers, the thickness of a sample film should be in closed thickness order. In some cases, it will be impossible to prepare the sample with such a thin film (under 1μm). For example, in the metal sector or silicon materials, it is

Peer-reviewed version available at Polymers 2020, 12, 1142; doi:10.3390/polym12051142

very hard to prepare a thin film under 1μm by using microtome. To overcome this drawback, Baden et al.[105] has adopted a new approach by using the Focused Ion beams (FIB) processing for thin sectioning sample instead of microtome. Although this method may lead to several deteriorations of the substrates due to the ion bombardments attacks and local thermal heating. However, the damages on the studied polymer surface (polyimide) by ion beam irradiation were negligible and the chemical structure of polyimide before and after treatment with FIB remains mostly unchanged. This kind of information is very interesting because it helps to overcome the drawbacks of this new technique at least with polyimide. The analysis of ultrafine thin needs higher sensibility equipment. For this purpose, a new resonance enhanced method to increase the sensibility of AFM-IR by using the Lorentz Contact Resonance (LCR) imaging mode is proposed.

With this improvement, it is possible to perform nanoscale IR spectroscopy on extremely thin films to even 5 nm thick. In other words, with the new devices, AFM-IR (NanoIR2s, nanoIR3) could able to investigate single polymer lamellae, self-assembled monolayers and biological membranes. Recently, Ni et al.[106] developed also a new setup based on time-resolved broadband Nano-IR using antenna-based near-field spectroscopy. In this approach, AFM tip was illuminated by a focused IR probe beam (Figure 6a) with probe beam spans frequencies of 830 - 1000 cm^{-1} [107](Figure 6b) which will generate strong evanescent electric fields beneath the tip. The monolayer graphene is covered by double layers of hexagonal boron nitride (h-BN), used as Plasmon doped material. These fields possess a wide range of in-plane momenta q and therefore facilitate efficient coupling to graphene Plasmon. This enhancement allows the detection of graphene Plasmon peak under photo-excitation and being able to analyze the mono-crystal of grapheme protected by an ultrathin (10 nm) layer of hexagonal boron nitride (hBN).

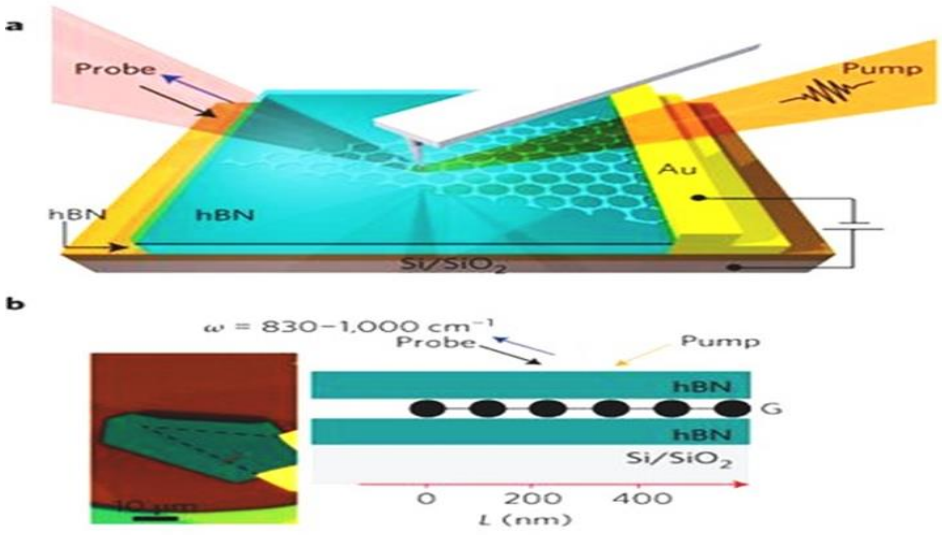

Figure 6. (a) The pump–probe nano-IR set-up and optical image of the hBN/G/hBN device; (b) the black dotted lines mark the graphene layer that is covered by two thin hBN layers. Adapted from G. X. Ni et al.,Nature Photonic, 2016, 10, 244-247. Copyright 2016 Nature publishing group.

The sensibility of AFM-IR can be also improved by using quantum cascade laser (QCL) [44, 108] and tuned the repetition rate of the QCL to match one of the contact modes resonance frequencies of the AFM cantilever, demonstrating a spatial resolution better than 50 nm[108]. Subsequently, they

Peer-reviewed version available at Polymers 2020, 12, 1142; doi:10.3390/polym12051142

further used a sharp gold-coated AFM tip and a gold-coated substrate with top-down illumination configuration, achieving the sensitive measurement of self-assembled monolayers and a spatial resolution of about 25 nm[44]. This technique, now referred to as resonance enhanced AFM-IR (RE-AFM-IR), allows performing more sensitive measurements compared to the original AFM-IR.

Recently, Dazzi et al. introduced the tapping of AFM-IR as a complement to AFM-IR in the contact mode, extending the application of AFM-IR to the soft or loosely adhesive samples such as polymeric nanoparticles and liposomes that are challenging for investigating, using AFM-IR in the contact mode[53, 109, 110]. In tapping AFM-IR, the tip off the AFM cantilever oscillates in tapping mode as traditional AFM. This method does not lead to the damage or removal of the sample when the tip scans across the surface of soft samples as seen in the AFM in contact mode. The spatial resolution of tapping AFM-IR with a heterodyne detection scheme on the soft samples was achieved to 10 nm[53, 109]. The principle of the tapping AFM-IR is based on heterodyne AFM[111-113] where the heterodyne detection scheme is achieved by setting the repetition rate of the laser to the difference between the first and the second Eigen modes of the AFM cantilever, tapping oscillation at the first mode and measuring at the second mode[53, 109]. The amplitude of the second mode is proved to be proportional to the absorbance[109] , thus the spectra obtained by the tapping AFM-IR correspond to traditional FT-IR spectra in terms of peak position and intensity.

3.2 Thermal Analysis (nano-TA)

The other significant feature of AFM about its attitude to be coupled with thermal analysis to better characterize thermal properties of heterogeneous samples in different regions. Also recognized as nano-thermal analysis (nano-TA), this groundbreaking AFM-related method enables a local thermometric analysis[114].

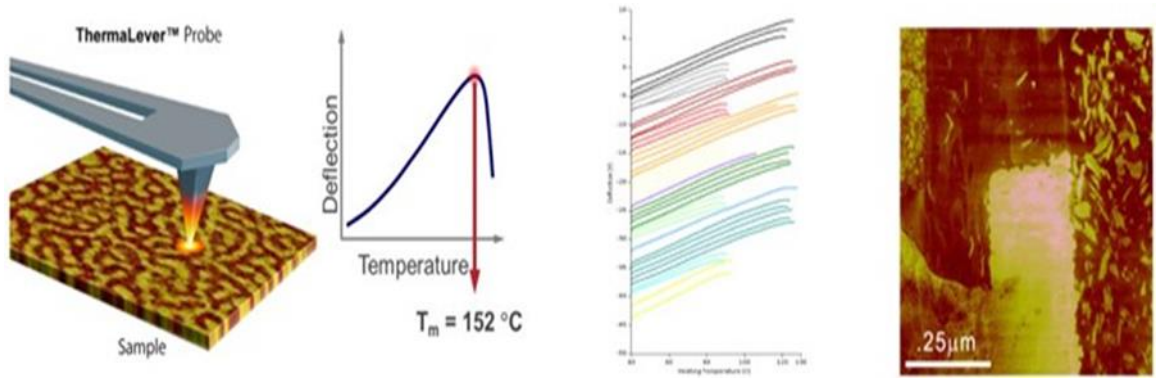

Figure 6. Left: nano-TA uses a heated AFM tip to measure glass transition and melt temperatures with nanoscale spatial resolution. Middle: Thermal transition curves on a 21 layer laminated polymer film. Right: Scanning thermal microscopy visualizes variations in temperature and thermal conductivity on a sectioned circuit board (Adapted from Anasys Instruments, Nanoscale thermal analysis, 2018).

The main advantage of testing nano-scale thermal analyzes is the detection of changes in the polymer crystal state in terms of glass transition temperature (T_g) and melting temperature (T_m), without affecting on its mechanical properties. This is achieved at the end of an AFM probe by using a special tip. During the measurements, the cantilever is heated while the probe is moved toward the

Peer-reviewed version available at Polymers 2020, 12, 1142; doi:10.3390/polym12051142

specimen until its expansion due to the cantilever is local heating (Figure 6). The sample swelling pushes the probe up and causes a rise in the vertical bending of the cantilever. Therefore, this deflection is assessed applying AFM photo-detector device based on an AFM standard. The specimen undergoes a change in internal temperature due to the transition temperature, being softer than the initial state; as a result, the cantilever bending decreases and the sample is forced to induce elastic or plastic deformation[114].

The product thermal transition can be determined by measuring the deflection of the cantilever. Furthermore, through this technique the sample's transition temperature can be positively correlated with the bulk measurements of the transition temperature obtainable with macroscopic thermal approach (i.e., thermomechanical and calorimetric analysis). Contrary to the bulk techniques, the nano-TA enables micro- and nano-scale analysis of local thermal properties of a sample. Therefore, this method will be certainly be used to identify the thermal behavior of specific polymers and/or biomaterials. The cantilever is typically made of silicon with different doses of dopants, whereas the probe is a standard etched silicon probe, which allows examinating high spatial resolution in both tapping and contact modes. The cantilever can reach very high temperatures in this configuration because silicon doping allows it to operate with high currents. It can therefore be argued that this technique is suitable for various polymers at wide range of temperatures [115]. Bozec and Odlyha reported using a thermal probe at the end of an AFM cantilever to analyze the denaturation of collagen fibrils [116].

Nguyen Tri et al. [117] reported in a recent publication on the nanoscale characterization of the structure of milkweed fibers that have special properties due to their superlight weight, natural super hydrophobic and hollow properties. In combination with high-resolution SEM, AFM-IR investigates the morphology and chemical composition of milkweed fibers at the nanoscale in order to provide a better understanding of their structure, especially on the fiber surface [118]. AFM-IR provide several tens of nanometer resolution surface mapping. AFM-IR's main limitation is the laser source near the infrared region (900–4000 cm^{-1}). It is not possible to detect bonding signals between polymer and metals below 900 cm^{-1}[118].

5. Application of AFM-IR in crystallization of polymer blends and polymer science

With numerous potential advantages by combining a nanoscale morphological characterization and chemical composition identification, the AFM-IR is a very useful tool for chemical characterization of a variety of materials, especially for structure-property relationship. We describe here the latest progress in the application of this technique to identify, verify the miscibility, interaction, aging and crystallization of polymer as well as related phenomena, which cannot be done with traditional AFM [107] and the information of these analyst are limited in the literature.

4.1. AFM-IR in crystallization of polymer blends

For blend materials, the understanding direct determination of the miscibility, the phase separation, the crystallization mechanism and the chemical interactions of components in a formulation is crucial to control their morphology and properties. However, its remain key challenges due to the lack of correlated imaging tool at sub nanometer and chemical characterization. The first application of AFM-IR in polymer blends that should be mentioned was the work of Prater

et al.[119] in which they tried to use AFM-IR to characterize a tertiary blend of common commercially polymers including polycarbonate (PC), epoxy resin (ER), polystyrene (PS). The AFM-IR provided IR spectra series in the C-H stretch region at 333 nm at different positions on the sample surface. The obtained results showed changes in terms of peak intensities of the CH peak between 2920 and 2970 cm^{-1} since the tip moved from PC to PS domains. Polycarbonate (PC)/ Acrylonitrile butadiene styrene (ABS) blends are one of the most popular materials used automotive and electronics devices thank to excellent properties including high flow for molding, heat resistance and toughness. AFM-IR can be used to explore deflection of PC/ABS blends by tuning the IR source to a fixed wavenumber and then scanning the sample.[120].The characterization and the distribution of polymer in ABS/PC was performed by recording the nano-IR spectra in the CH stretching region between 3200 and 2800 cm^{-1}. The spectra is scaled to the IR band at 3028 cm^{-1}, which is due to an aromatic C-H stretching vibration of polystyrene (PS). The IR intensity of CH_3 stretching band at 2960 cm^{-1} assigned to PC and CH_2-stretching band at 2932 cm^{-1} assigned to polystyrene (PS) exhibit significant changes when the AFM cantilever was scanning on sample surface and thus can provide chemical composition of ABS/PC at the nanoscale[120].

Felts et al.[121, 122] have been conducted researches on investigation of tip-based nanofabrication, chemical identification, and nanometer-scale chemical imaging of polymer nanostructures with over 100 nm spatial resolution for several polymer systems including polyethylene (PE), polystyrene (PS), and poly (3-dodecylthiophene-2, 5-diyl)(PDDT). The polymer nanostructures were written near similar substrate, with some nanostructures overlapping. The position of absorption peaks at the 2926 cm^{-1} band assigned to asymmetric C-H stretch and at the 2860 cm^{-1} band assigned to symmetric C-H stretch respectively can be shifted to lower or higher frequency with a variation of feature sizes. This is because the thermal expansion of polymer blends depends on feature size and thus the cantilever response amplitude decreases as the polymer feature size decreases. In the case of PS and PDDT, although AFM-IR spectra show a low signal-to-noise, due to artifacts of laser power drift, the authors can still distinguish between nanostructures of PE, PS, and PDDT[121, 122].

The determination of miscibility of amorphous components in polymer blends used in pharmaceutical systems was also investigated by AFM-IR. Van Eerdenbrugh et al.[67, 123] used a standard atomic force microscopy (AFM) measurements combined with nanoscale mid-infrared (mid-IR) spectroscopy to evaluate the miscibility of an equimolar binary blend between poly-(vinylpyrrolidone) (PVP) with dextran or maltodextrin (DEX). By analyzing IR absorption peaks at 1280 and 1350 cm^{-1}, it is possible to distinguish between rich-DEX or rich-PVP domains. More specifically, for pure DEX, the intensity of the 1350 cm^{-1} band was often higher than that of the 1280 cm^{-1} band, while for PVP, the opposite tendency was observed. The AFM-IR results showed that the large discrete domains correspond to DEX-rich phases, while the continuous phase is rich in PVP, with a good agreement between the topographical and the chemical images.

In the petroleum and natural gas industry, the use of hydraulic fracturing technique to crack rock is one of the most popular methods to release oil or natural gas by using sealing materials capable of performing under ultra-high temperature high pressure (Ultra HTHP)[124]. These materials were often fabricated by a blend of high-performance materials including perfluoro-elastomers (FFKMs), polyaryletherketones (PEEK etc.), polytetraflouroethylenes (PTFE) and ethylene–propylene diene monomer (EPDM) rubber. A good understanding the compatibly, the

Peer-reviewed version available at Polymers 2020, 12, 1142; doi:10.3390/polym12051142

micro, nanostructure and the chemical properties of the blend is the key factor to improve their design and their process development93. AFM-IR spectra helped chemical identification of each pure polymer component in the blend and thus can help to optimize the blending conditions[124]. That means AFM-IR spectroscopy and imaging provides information to control the convergence of processing conditions and thus to obtain a desirable mixing to better performance of the end-use polymer[90].

Hitesh et al.[66] investigated the miscibility of the drug-polymer amorphous solid dispersion (ASDs) of Iitraconazole (ITZ) and hydroxypropylmethylcellulose (HPMC) blend using the AFM-IR and fluorescence. They indicated that both AFM-IR and fluorescence imaging were able to provide information about the microstructure of the ASDs, prepared by solvent evaporation and the phase separation occurred at the submicron scale. When the films were heated, it was observed that the ASD components underwent mixing. Authors affirmed that the AFM-IR are promising for the characterization of miscibility and microstructure in drug-polymer systems. The phase behavior of blends of a pair of partially miscible polymers, poly(vinylpyrolidone) (PVPK90) and hydroxypropyl methylcellulose acetate succinate (HPMCAS) to fabricate of nanofibers for tunable drug delivery and nanoscale phase separation in electrospun blend fibers was confirmed by interpreting of AFM-IR data[125].

Recently, the miscibility of a polymer blend based on telaprevir with three different polymers, an amorphous solid dispersions drug, was evaluated using nanoscale infrared spectroscopy, thermal analysis, and Lorentz contact resonance measurements[126]. Author indicated that, the AFM-IR is very useful to characterize the microstructure of solid dispersion as a function of polymer nature and to determine phase separation. The AFM-IR results show that drug-rich phase was found to form discrete domains of various sizes depending on the system, ranging from below 50 nm to a few hundred nanometers, whereas the continuous phase was polymer-rich[126]. The AFM-IR has used to identify the nature of spherulitic and polymeric separation in the blend. Figure 7 show an example of AFM image (Figure 7a) and AFM-IR image at the 1720 cm^{-1} band (Figure 7b) of the equimolar blend between polycaprolactone (PCL) and polyethylene glycol (PEG). The image of the carbonyl band at 1720 cm^{-1} is very useful to identify the distribution of PCL in the blend[127].

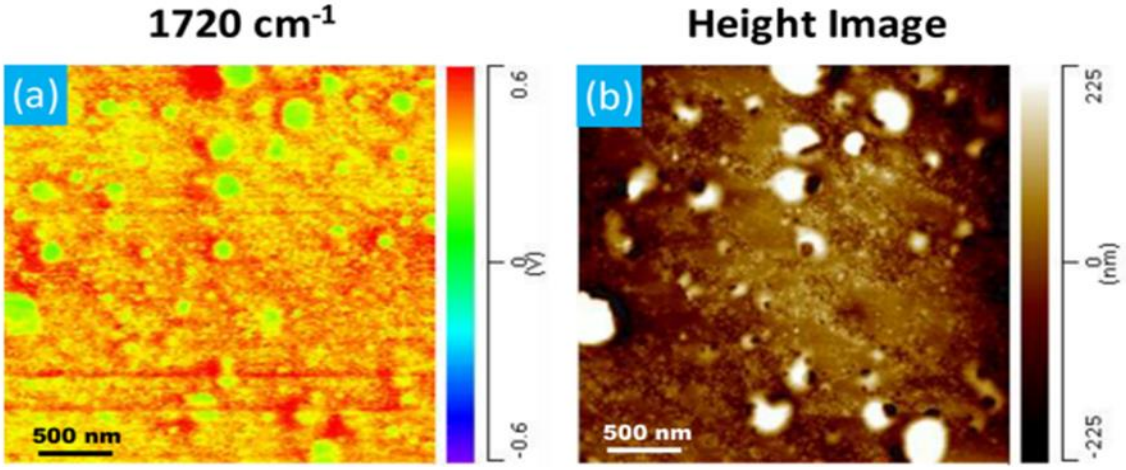

Peer-reviewed version available at Polymers 2020, 12, 1142; doi:10.3390/polym12051142

Figure 7. PCL/PEG (50/50) blend, quickly quenched in liquid nitrogen upon crystallization temperature at 40 °C from the melt: (a) chemical image of the 1720 cm^{-1} band, (b), AFM image (Adapted from P. Nguyen Tri, Macromolecules 2018, 51, 7266−7273.

Tang 2016 et al.[65] used the AFM-IR to characterize compositions of nanodomains in a commercial high-impact polypropylene. These alloys consist mainly of polypropylene but possibly a small amount of polyethylene (PE) homopolymers, as well as ethylene-propylene random copolymer (or ethylene-propylene rubber, EPR) and ethylene-propylene block copolymers (EbP)[65]. These materials possess multi-level phase structures and contain core-shell rubber particles with internal structures dispersed in a continuous PP matrix, with the order of several hundred nanometers. The chemical characterization of this core-shell is impossible with a traditional FT-IR. By using the AFM-IR, compositions of different phase domains in a commercial HIPP have been determined quantitatively and author affirmed that the major component of the rigid cores in the rubber particles of the HIPP is PP, not PE as previous described before. More recently, they published also a similar work on the use of both nano-TA and AFM-IR to investigate the chemical composition and structure of a high impact polypropylene (HIPP)[128].

4.1.1. Effect of film thickness

The glass transition temperature (Tg) of polymer films decreases with decreasing film thickness[129, 130], which could cause the thin polymer films begin to relax at a temperature far below the value for bulk metric[130]. Relaxation behavior and T_g depression with film thickness decreasing in thin polymer films have limited their applications in many cases. For example, when thin polymer films are employed as dielectrics in micro or nano devices, the dielectric loss could occur far before the breakdown of the thin polymer films [131].Yang et al. using AFM measured the viscosity of unentangled, short-chain polystyrene (PS) films on silicon substrate at different temperatures and found that the transition temperature for the viscosity decreased with the decreasing film thickness[132]. Atomic force microscopy (AFM) has been used recently as an invasive measurement technique to straightforwardly determine the absolute thickness of polymer films. Among all surface analysis techniques, AFM has the highest vertical resolution of less than 0.1 nm for most commercial systems[133].

To follow crystallization and melting of most polymers, it is necessary to have control over sample temperature. The development of stable controlled temperature accessories to AFMs has allowed a wide range of polymers to be imaged during crystallization at temperatures from 0 °C to 250 °C [81, 134-136]. Environmental control, with the use of both vacuum and inert gas atmospheres[136, 137], has allowed polymers that are susceptible to oxidation and hydrolysis to be studied at high temperature.

Following crystallization in many polymers with AFM is limited to temperatures close to Tg or T_m, where crystal growth is slow. Recently a novel high speed scanning AFM was developed, Video FM, which allows images to be collected at video rate[137, 138].

4.1.2 Effect of blend composition

AFM–IR is now being used in extensive applications in polymer science. A driving factor is the number and diversity of polymeric materials that incorporate micro-and nanoscale structure to

Peer-reviewed version available at Polymers 2020, 12, 1142; doi:10.3390/polym12051142

achieve desired properties. Such materials include polymer blends, polymer composites and nanocomposites, and thin films used in both active devices and as passive barriers. Figure 8 shows a proprietary multicomponent polymer blend. Blends with micro- and nanoscale-sized polymer domains are increasingly common. Often different combinations of polymers are used to achieve desired strength, toughness, and other performance criteria for a specific application. AFM–IR can reveal the spatial distribution of these polymer components and chemically identify polymer constituents[107].

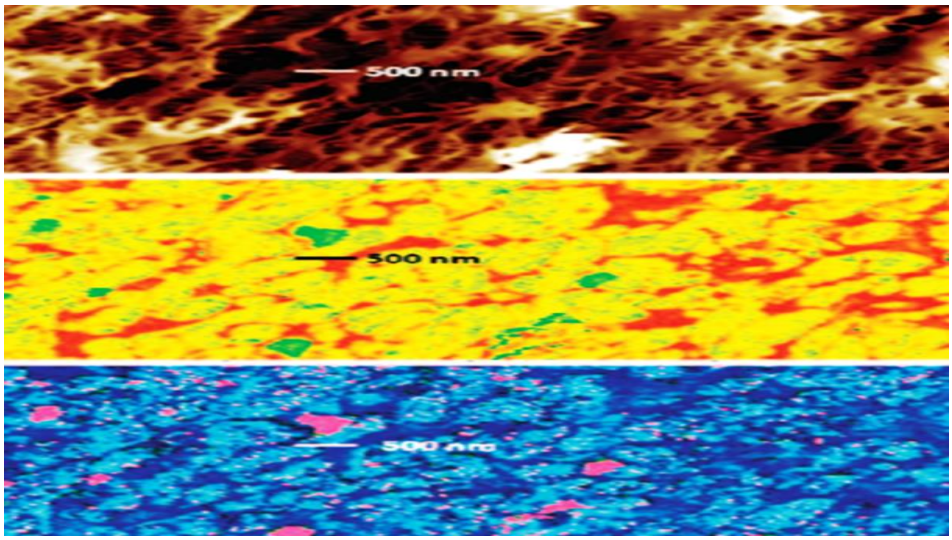

Figure 8. AFM–IR measurements of a polymer blend, including topography image (top), IR absorption at 1450 cm^{-1} (center), and stiffness map (bottom). Adapted from: Alexandre Dazzi et al 66 (12), 1365-1384 (2012).

4.2 AFM-IR in studying crystallization of miscible blends

In the miscible crystallizable blends, the determination of the polymer distribution becomes more complex because it cannot do with morphological tools. The examination of the polymer distribution in miscible blends, particularly at the sub-micrometer level, is a technically unfeasible task despite the recent advances in several microscopies and X-ray techniques [139-142]. AFM-IR has been used to investigate the crystallization behavior and the diffusion in crystalline/crystalline blends of polyethylene glycol (PEG) with poly(3-hydroxybutyrate) (PHB). The addition of PEG helps to improve the biodegradation of PHB and extends their applications. However, the presence of PEG will perturb the crystallization of the PHB. The polymers form a miscible blend, the PHB with the higher melting temperature crystallizes first and the lower-T_m PEG component is trapped between the lamellae of the high-T_m component in a two-step crystallization process[143].

To investigate the distribution of each polymer in the spherulitic structure, they take advantage that PHB and PEG have different IR characteristics: PHB exhibits a strong absorption band at 1720 cm^{-1}, assigned to the stretching vibration of the carbonyl groups, whereas the IR spectrum of PEG does not exhibit this peak. In contrast, a strong band at 1095 cm^{-1}, which is assigned to the stretching vibration of the C-OH groups, is observed in the PEG spectrum but is negligible in the PHB spectrum. The bands at 1720 and 1095 cm^{-1} are thus chosen to identify the presence of PHB and PEG, respectively, in their blends. The crystallization of the blend was also conducted at 40 ºC, below the melting point

Peer-reviewed version available at Polymers 2020, 12, 1142; doi:10.3390/polym12051142

of PEG (about 59 ºC), allowing the crystallization of both polymers in a process of competitive crystallization and segregation. Figure 9a shows a POM image of the PHB/PEG (50/50) blend, isothermally crystallized at 40 ºC. It shows the presence of two types of spherulites, denoted A and B. Spherulites A already appear during the cooling as shown in Figure 9b, they are banded with a ring spacing of 12-15 μm; they are attributed to the crystallization of PHB. In contrast, spherulites B appear at 40 °C; they are small and non-banded as shown in Figure 9c. They are cone-like and were attributed to the crystallization of both PHB and PEG [144].

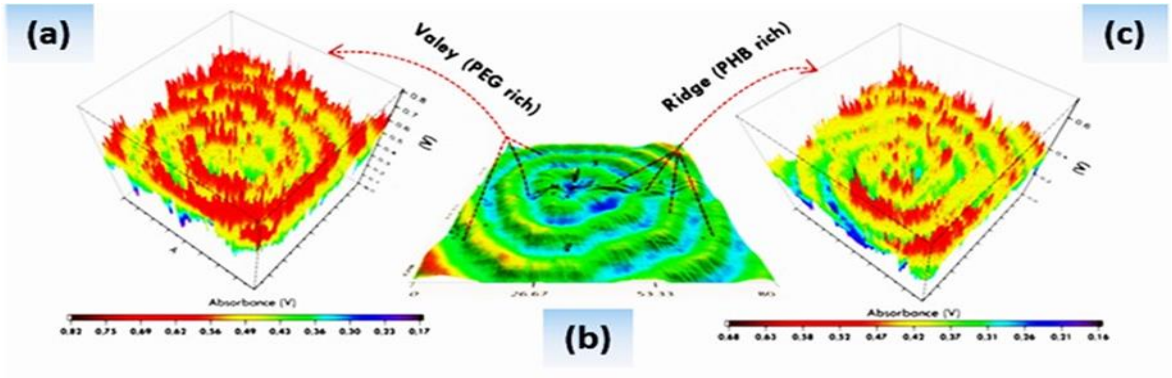

Figure 9. The PHB/PEG (50/50) blend isothermally crystallized at 40 ºC: a) tridimensional chemical image at the 1720 cm-1 band; b) tridimensional AFM image and c) tridimensional chemical image at the 1095 cm^{-1} band. Adopted from; P. Nguyen-Tri, Macromolecules, 2018, 51 (1), 181-188. Copyright 2018 American Chemical Society.

4.3 AFM-IR in studying crystallization of immiscible blend

There are some works reported in the literature on the use of AFM-IR to investigate the crystallization behavior and the diffusion polymer in the complex systems, including equimolar miscible and immiscible crystalline/crystalline blends at the nanoscale [127, 144-147]. They used AFM-IR to analyze the crystallization behavior of an immiscible biopolyester based on polycaprolactone (PCL) and polyethylene glycole (PEG). The crystallization of this system is complex because they have very similar melting temperature T_m and thus is expected to have the simultaneous crystallization. However, by variation of crystallization conditions (temperature, composition), a great discrepancy of crystallization kinetics can be obtained. During the quenching from the melt, this system exhibits a contention between the liquid-liquid phase separation and crystallization. However, the polymer phase separation at the nanoscale and the distribution of polymer in the sub-micrometer structure are limited and thus the mechanism of the crystallization process is still not fully understood. The crystallization of an equimolar blend is first carried out at different temperatures between 30 and 40 ºC near the melting temperature and followed the technic of polarized optical microcopy (POM).

It demonstrates that when the crystallization temperature goes lower than 37.5 ºC, the crystallization has undergone in two steps. The first polymer crystallizes first to form spherulites and then suddenly, the nucleus of another polymer appears in the boundary of spherulites of the first polymer and grows perpendicularly to the interface. The crystals of the second polymer cannot develop to spherulitic structure. When the temperature is higher than 37.5 ºC, one step crystallization is observed. The transition from two steps to one step crystallization is perceived at 37.5 ºC where both inside and outside rejection are found. To identify the nature of each polymer in the blend, the

AFM-IR spectrum of each pure component is first measured to determine the characteristic peak of each polymer. In this case, PCL exhibits a strong peak at about 1725-1728 cm^{-1} due to the presence of carbonyl group, while this peak is absent in the PEG[127].

4.4 Other applications of AFM-IR in polymer science

With numerous potential advantages by combining a nanoscale morphological characterization and chemical composition identification, the AFM-IR is a very useful tool for chemical characterization of a variety of materials, especially for structure- property relationship. Some the latest progress in the application of this technique to identify, verify the miscibility, interaction and aging as well as related phenomena which cannot be done with traditional AFM are described here [60].

4.4.1. AFM-IR in identification of polymer blends

For blend materials, the understanding direct determination of the miscibility, the phase separation, the crystallization mechanism and the chemical interactions of components in a formulation is crucial to control their morphology and properties. However, there remain many key challenges due to the lack of correlated imaging tool at sub nanometer and chemical characterization. The first application of AFM-IR in polymer blends that should be mentioned was the work of Prater et al.[148]. They tried to use AFM-IR to characterize a tertiary blend of common commercially polymers including polycarbonate (PC), epoxy resin (ER), polystyrene (PS). The AFM-IR provided IR spectra series in the C-H stretch region at 333 nm at different positions on the sample surface. The obtained results showed changes in terms of peak intensities of the CH peak between 2920 and 2970 cm^{-1} since the tip moved from PC to PS domains. Polycarbonate (PC)/ Acrylonitrile butadiene styrene (ABS) blends are one of the most popular materials used automotive and electronics devices thank to excellent properties including high flow for molding, heat resistance and toughness. AFM-IR can be used to explore deflection of PC/ABS blends by tuning the IR source to a fixed wavenumber and then scanning the sample. The IR absorption and stiffness then could be obtained directly by measuring the amplitude of the nano-IR signal and the frequency of the fundamental contact resonance respectively[120].

The characterization and the distribution of polymer in ABS/PC is performed by recording the nano-IR spectra in the CH stretching region between 3200 and 2800 cm^{-1}. The spectra is scaled to the IR band at 3028 cm^{-1}, which is due to an aromatic C-H stretching vibration of polystyrene (PS). The IR intensity of CH3 stretching band at 2960 cm^{-1} assigned to PC and CH2-stretching band at 2932 cm^{-1} assigned to polystyrene (PS) exhibit significant changes when the AFM cantilever was scanning on sample surface and thus can provide chemical composition of ABS/PC at the nanoscale[120].

Felts et al. [121, 122] have been conducted researches on investigation of tip-based nanofabrication, chemical identification, and nanometer-scale chemical imaging of polymer nanostructures with over 100 nm spatial resolution for several polymer systems including polyethylene (PE), polystyrene (PS), and poly (3-dodecylthiophene-2, 5-diyl)(PDDT). The polymer nanostructures were written near same substrate, with some nanostructures overlapping. The position of absorption peaks at the 2926 cm^{-1} band assigned to asymmetric C-H stretch and at the 2860 cm^{-1} band assigned to symmetric C-H stretch respectively can be shifted to lower or higher frequency with a variation of feature sizes. This is because the thermal expansion of polymer blends

Peer-reviewed version available at Polymers 2020, 12, 1142; doi:10.3390/polym12051142

depends on feature size and thus the cantilever response amplitude decreases as the polymer feature size decreases. In the case of PS and PDDT, although AFM-IR spectra show a low signal-to-noise, due to artifacts of laser power drift, the authors can still distinguish between nanostructures of PE, PS, and PDDT [121, 122].

The determination of miscibility of amorphous components in polymer blends used in pharmaceutical systems was also investigated by AFM-IR. Van Eerdenbrugh et al [67, 123] used a standard atomic force microscopy (AFM) measurements combined with nanoscale mid-infrared (mid-IR) spectroscopy to evaluate the miscibility of an equimolar binary blend between poly-(vinylpyrrolidone) (PVP) with dextran or maltodextrin (DEX). By analyzing IR absorption peaks at 1280 and 1350 cm^{-1}, it is possible to distinguish between rich-DEX or rich-PVP domains. More specifically, for pure DEX, the intensity of the 1350 cm^{-1} band was often higher than that of the 1280 cm^{-1} band, while for PVP, the opposite tendency was observed. The AFM-IR results showed that the large discrete domains correspond to DEX-rich phases, while the continuous phase is rich in PVP, with a good agreement between the topographical and the chemical images.

In the petroleum and natural gas industry, the use of hydraulic fracturing technique to crack rock is one of the most popular methods to release oil or natural gas by using sealing materials capable of performing under ultra-high temperature high pressure (Ultra HTHP)[124]. These materials are often fabricated by a blend of high-performance materials including perfluoro-elastomers (FFKMs), polyaryletherketones (PEEK etc.), polytetraflouroethylenes (PTFE) and ethylene–propylene diene monomer (EPDM) rubber. A good understanding the compatibly, the micro, nanostructure and the chemical properties of the blend is the key factor to improve their design and their process development. AFM-IR spectra helped chemical identification of each pure polymer component in the blend and thus can help to optimize the blending conditions[124].That means AFM-IR spectroscopy and imaging provides information to control the convergence of processing conditions and thus to obtain a desirable mixing to better performance of the end-use polymer[124]

Hitesh et al.[66] et al. investigated the miscibility of the drug-polymer amorphous solid dispersion (ASDs) of itraconazole (ITZ) and hydroxypropylmethylcellulose (HPMC) blend using the AFM-IR and fluorescence. They indicated that both AFM-IR and fluorescence imaging were able to provide information about the microstructure of the ASDs, prepared by solvent evaporation and the phase separation occurred at the submicron scale. When the films were heated, it was observed that the ASD components underwent mixing. Authors affirmed that the AFM-IR are promising for the characterization of miscibility and microstructure in drug-polymer systems.

The phase behavior of blends of a pair of partially miscible polymers, poly(vinylpyrolidone) (PVPK90) and hydroxypropyl methylcellulose acetate succinate (HPMCAS) to fabricate of nanofibers for tunable drug delivery and nanoscale phase separation in electrospun blend fibers was confirmed by interpreting of AFM-IR data[125].

Recently, the miscibility of a polymer blend based on telaprevir with three different polymers, an amorphous solid dispersions drug, was evaluated using nanoscale infrared spectroscopy, thermal analysis, and Lorentz contact resonance measurements[126]. Author indicated that, the AFM-IR is very useful to characterize the microstructure of solid dispersion as a function of polymer nature and to determine phase separation. The AFM-IR results show that drug-rich phase was found to form discrete domains of various sizes depending on the system, ranging from below 50 nm to a few hundred nanometers, whereas the continuous phase was polymer-rich[126].

Peer-reviewed version available at Polymers 2020, 12, 1142; doi:10.3390/polym12051142

The AFM-IR has used to identify the nature of spherulitic and polymeric separation in the blend. Figure 10 show an example of AFM image (Figure 10a) and AFM-IR image at the 1720 cm^{-1} band (Figure 10b) of the equimolar blend between polycaprolactone (PCL) and polyethylene glycol (PEG). The image of the carbonyl band at 1720 cm^{-1} is very useful to identify the distribution of PCL in the blend[93].

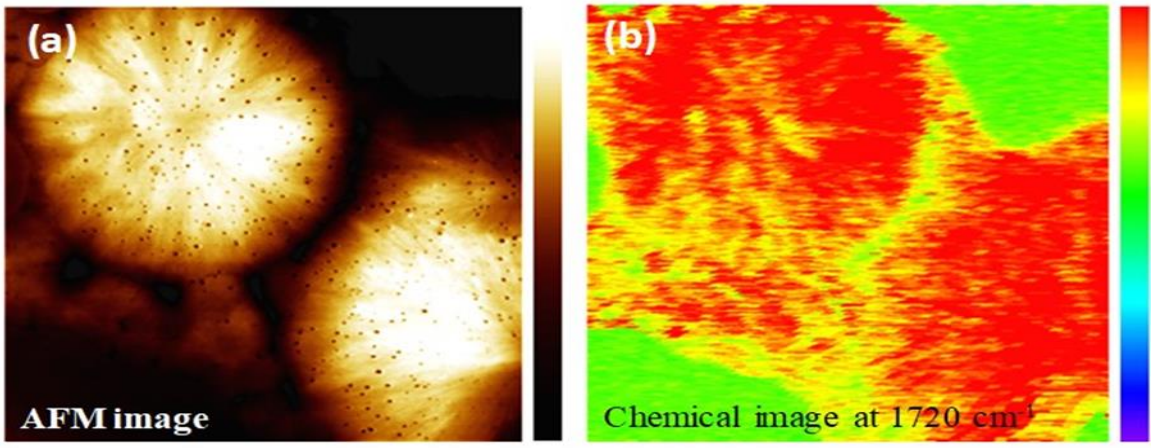

Figure 10. PCL/PEG (50/50) a) AFM image and infrared image at the 1720 cm-1 band, showing the distribution of PCL in the blend.

Tang et al.[65] used the AFM-IR to characterize compositions of nanodomains in a commercial high-impact polypropylene. These alloys consist mainly of polypropylene but possibly a small amount of polyethylene (PE) homopolymers, as well as ethylene-propylene random copolymer (or ethylene-propylene rubber, EPR) and ethylene-propylene block copolymers (EbP)[65]. These materials possess multi-level phase structures and contain core-shell rubber particles with internal structures dispersed in a continuous PP matrix, with the order of several hundred nanometers. The chemical characterization of this core-shell is impossible with a traditional FT-IR. By using the AFM-IR, compositions of different phase domains in a commercial HIPP have been determined quantitatively and author affirmed that the major component of the rigid cores in the rubber particles of the HIPP is PP, not PE as previous described before. More recently, they published also a similar work on the use of both nano-TA and AFM-IR to investigate the chemical composition and structure of a high impact polypropylene (HIPP)[65].

For composite materials, the chemical characterization in the interfacial region between polymer matrix and reinforcements is very important to better understanding the final properties and the failure mechanisms during the service lifetime of polymeric materials. The latter may help formulation converge more efficiently on optimal processing conditions. AFM-IR has proven to be a useful tool for this kind of analysis processing conditions. AFM-IR has shown to be a useful tool for this kind of analysis.

4.4.3. AFM-IR in biopolymers and multilayers

Nowadays, biopolymers are growing in importance and current research is focused on producing newer polymers. Many bio-resourced based polymers have been synthesized or are formed in nature during the growth cycles of all organisms. The increasing number of publications during recent years reflect the growing importance of these new materials. The application of a new

Peer-reviewed version available at Polymers 2020, 12, 1142; doi:10.3390/polym12051142

technique or method like AFM-IR to analyze morphology, properties and structure of these materials is attracting the attention of the scientific community.

Mayet C et al.[162] investigated the production of bacterial polyhydroxybutyrate in Rhodobacter capsulatus using transmission electron microscopy (TEM) and AFM-IR. They concluded that AFM-IR was more useful and takes less time to prepare the sample compared to TEM. The Samples can be ready for a detailed analysis after 1 day of preparation instead of 2-3 weeks for TEM analysis. The other advantages of AFM-IR relates to its capacity to obtain chemical images and can directly identify the presence of the PHB in blends by analyzing AFM mapping image at the 1740 cm^{-1} band, assigned to carbonyl group, while the TEM images were not able to do that. AFM-IR was also used to study the interface of a laminated multilayer film based on Ethylene Acrylic Acid (EAA) copolymer/Polyamide (nylon) blend. Compared to traditional FTIR having a special resolution of around 10 μm, the use of AFM-IR shows clearly better resolution at the interface. It was interesting to show that there was a very good correlation between IR spectra of polymer measured by bulk traditional FTIR measurements and AFM-IR[60].

Gong L et al[64] used AFM-IR technique to investigate morphological and structural details of individual electronspun nanofibers of poly[(R)-3-hydroxybutyrate-co-(R)-3-hydroxyhexanoate] (PHBHx) collected across the air gap on aluminum foil and on the tapered edge of a high-speed rotary disk. They indicated that the IR peak in AFM-IR are in good agreement with traditional FTIR in terms of peak/shoulder position and relative intensity but more highly resolved compared to those of traditional FT-IR and it thus facilitates the result analysis. By using AFM-IR combined with other characterization techniques such as wide-angle X-ray diffraction (WAXD), Selected Area Electron Diffraction (SAED), authors have proposed, for the first time, a new generation mechanism of β-form crystal structure in the interface, never before identified, and different with (to) those previously reported.

Recently, Kelchtermans et al. [72] have used AFM-IR to characterize polyethylene-polyamide (PE-PA) multilayer films. Authors indicated that a two-mm-thick barrier layer between two polyamide layers near the center of the multilayer film consists of an ethylene-vinyl alcohol copolymer and this contention was proven by mechanical stiffness and thermal property measurements. They also confirmed that in thin tie layers, even less than several micrometers thick, the assignment of the components in the laminate was readily obtained.

4.4.4. AFM in studying polymer aging

During the service lifetime the performance of polymers can deteriorate through the aging process due to environmental factors such as temperature, UV radiation and humidity [145, 147, 163-165]. This alteration can lead to the decommissioning of these products. The aging of polymer material is manifested in physical and chemical degradations, a slow and irreversible process. The effects of this degradation resulting from the notion of the "life time" of the material, i.e. the time required a property (physical, chemical, or electrical) to reach a threshold below which the material becomes unusable. The term physical aging encompasses all processes leading to irreversible alteration of the material properties without chemical modification of the structure of the macromolecules constituting the material. Physical aging [159] may result from: i) changes in the

Peer-reviewed version available at Polymers 2020, 12, 1142; doi:10.3390/polym12051142

spatial configuration of macromolecules (crystallization)-surface phenomenon; ii) surface phenomenon (cracking of the surfactant environment); iii) Transport phenomenon (solvent penetration, migration of adjuvants).

Chemical aging [122] relates to phenomena involving a chemical modification of the polymeric material under the influence of the environment. In practice, chemical aging often overlaps with physical aging and the two interferons Chemical aging[160]may relates from: i) changes in the spatial configuration of macromolecules (crystallization)-surface phenomenon; ii) surface phenomenon (cracking of the surfactant environment); iii) Transport phenomenon (solvent penetration, migration of adjuvants). Chemical aging[166] relates to phenomena involving a chemical modification of the polymeric material under the influence of the environment. In practice, chemical aging often overlaps with physical aging and the two interferons. Chemical aging [166] relates to phenomena involving a chemical modification of the polymeric material under the influence of the environment. In practice, chemical aging often overlaps with physical aging and the two interferences phenomena. The main general types of reaction involved in chemical aging are the following: scission of polymer chains, depolymerization, crosslinking, and oxidation. Understanding the aging mechanism is crucial because it can provide information on the prediction of service lifetime of polymer materials. This can help to avoid accidents due to the use of unsuitable polymers and to interfere with the aging process to accelerate or slow down the degradation. In this direction, investigations on the aging and stability of polymers are extensively realized. The recent advances in nanoscale analysis have shed lights to the aging investigations. Recently, AFM-IR has been used for better understanding the aging mechanism of common polymers and composites.

Morsch's group have shown several works on the use of AFM-IR to investigate the aging processes of several coatings and polymers[161], [167-171]. AFM-IR has been used to analyze the chemical composition of aging products on the surface of a composite based on epoxy resin and silicon rubber. They used the electrical discharge to attack the composite surface and then investigate its effect on the chemical composition of the composite in the surface by both ATR-IR and AFM-IR. In many cases, ATR-IR gives similar results in aged and non-aged samples, meaning that the aging process has no effect on the chemical structure of the composites. However, AFM-IR can provide more resolved spectra and nanoscale chemical mapping image of oxidative products (interfacial tracks and buries channels). The AFM-IF helps to confirm that the silicon rubber remains stable under these electrical attacks.

In another publication, they used both ATR-IR and AFM-IR to investigate the degradation of oil paint used in the Picasso and Mondrian paintings[170]. The ancient painting made from linseed oil with inorganic titanium white pigment particles was analyzed to identify the degradation of these materials with time. The characterization of oxidative products on the painting surface is found to be very useful for better understanding the degradation mechanisms and thus can be said to be the best method for better preserving these artworks[170].

The aging mechanism of a PET fiber under accelerated aging conditions is also reported [145]. Although, PET is a common polyester polymer and the aging mechanisms of this polymer have been extensively investigated. However, there are still open questions relating to this topic. About the distribution of oxidized functional groups on the fiber surface; the homogeneity of the polymer degradation on the surface at the nanoscale and molecular structure changes during the aging process

of PET. The main mechanisms of photo-oxidation of PET are related to the Norrish type I and the Norrish type II mechanisms[172, 173].

The degradation of PET via the Norrish type I mechanism leads to the formation of ketone radicals and to alkyl or aryl radicals around the ester linkage groups by splitting the molecule near the carbonyl bond; in turn, the Norrish type II mechanism involves an intramolecular reaction via a cyclic six-membered transition species and results in carboxylic end groups and alkenes. Although there are several studies on the accelerated weathering degradation of PET in thin films [174, 175], the degradation of PET fibers in a complex structure as filtration membranes has not been studied so far. Furthermore, due to limitations inherent in the characterization techniques used, the degradation studies are usually carried out on a macroscopic scale and the mechanism by which PET deteriorates upon accelerated weathering, especially on its surface at the nanoscale, is still an open question. AFM-IR is used to follow the aging process of PET fiber.

By analyzing at the nanoscale of the chemical composition and the distribution of functional groups appearing on the aged sample surface (Figure. 11), an understanding complementary of the mechanism of degradation under artificial weathering conditions has been proposed, in which hydrolysis and photo-oxidation processes via perester and aromatic acid species are mainly observed. At the molecular level, obtained results showed a transfer from the trans-conformer to the gauche conformer during the aging process, as shown by the increase of the characteristic IR bands of the gauche conformer at 1096 cm^{-1} and the decrease of the IR bands of the trans-conformer at 1340 cm^{-1}. In another case, AFM-IR is used to compare the mechanism of aging of an organic coating based on Polyurethane in two different conditions[147]: i) In natural exposure up to 10 years and ii) in accelerated conditions. The analyzed the distribution of carbonyl groups on the surface of both naturally and artificially aged samples. Two aging mechanisms have been observed. In the naturally exposed coating, the oxidized group developed from holes and crack borders to the bulk matrix and this process is inhomogeneous, while in the accelerated aging condition, the oxidized groups are homogeneously distributed on the whole surface without serious crack on the sample surface. From the kinetic data on properties and structural changes, authors have compared the results in the both cases and proposed models to calculate the service lifetime of these coating.

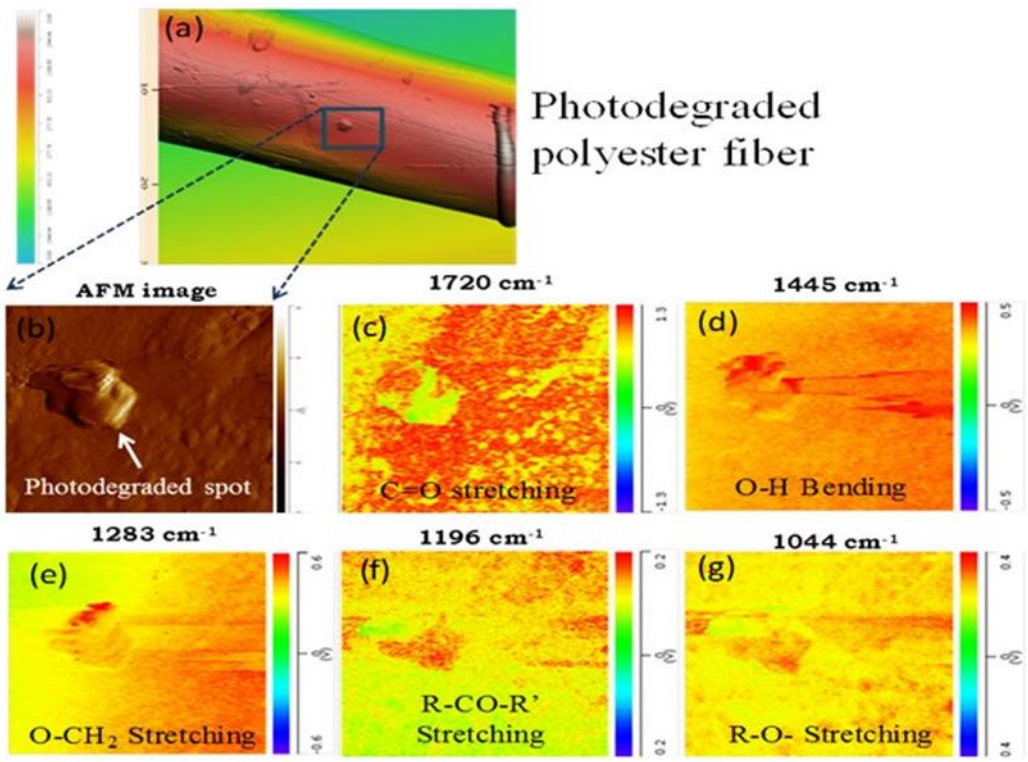

Figure 11. Tridimensional AFM height image (a) of an exposed PET fiber (500 h) and (b) of a high-resolution AFM image of the same fiber. High resolution IR mapping images (c–g) at different wavelengths: c) 1720 cm^{-1} (carbonyl stretching, crystalline); d) 1445 cm^{-1} (OH bending in carboxylic); e) 1283 cm^{-1} (O-CH2 stretching); f) 1196 cm^{-1} (R-COR'); and g) 1044 cm^{-1} (alkoxy, R-O). The dimension of the images (b–g) is 5 μm2. Reproduced from P. Nguyen-Tri et al., J. Photochem. Photobiol. A. Chem., 371, 2019, 196-204. Copyright 2019 Elsevier

5. Summary and outlook

This paper provides an overview of the use of atomic force microscopy to understand the crystallization of polymers. It has concentrated on the AFM observations and the wide and successful application of the AFM technique, as an adjunct to other methods, is beyond the scope of this article. Especially, AFM-IR dealing with polymer composites, polymer blends biopolymers and multilayers, polymer crystallization and polymer aging. With the improvement of the technology, AFM-IR has become a new technique for chemical analysis and compositional imaging with nanoscale spatial resolution of complex polymeric systems. Nano-TA is a useful for the identification of polymers and polymer blends with high precision at the nanoscale.

AFM-IR technique can obtain chemical images at selected wavelength or spectra at selected position, but the collection of a full IR spectrum has not yet been achieved. Additionally, the rapid developments of AFM-IR enable it to find numerous applications in many fields, especially suitable for materials with high thermal expansion coefficient, such as polymers and biomaterials. Materials with low expansion coefficient, such as inorganic materials or metallics, may be better analyzed by other nanoscale techniques. Nevertheless, thanks to the rapid developments and user-friendly operation of the AFM-IR, it is expected that publications about AFM-IR will increase significantly in the forthcoming years. In the polymer crystallization investigation, the improvement of spatial resolution of AFM-IR up to 10 nm will bring various additional advantages in analyzing chemical

composition of complex blends, especially for thin and ultrathin films. Much of the strength of AFM has been in confirming what was already 'known' about the structural evolution of polymers.

Peer-reviewed version available at Polymers 2020, 12, 1142; doi:10.3390/polym12051142

Biography of authors

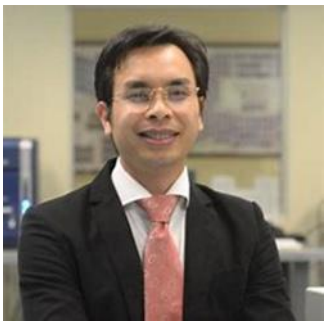

Phuong Nguyen-Tri is a regular Professor at University of Quebec à Trois-Rivieres (UQTR), Canada. He holds a Ph.D. degree at Cnam of Paris, France 2009. His main research interests are polymers, multifunctional composites, green chemistry, hybrid nanoparticles, smart coatings and nanoscale characterization of polymeric materials. Prof. Nguyen-Tri has edited of 10 Elsevier's books with the collaboration of over 300 internationally worldwide recognized researchers. He is also author of 11 book chapters, 3 patents and over 90 articles and conference proceedings including ACS and nature journals. He served as an editor of several special issues in ISI indexed journals. He is editorial board membership of several esteemed journals such as PLoS One (Q1, IF=2.9), SN Applied Science (Nature-Springer). He is currently international grants reviewer and a regular reviewer for over 30 journals from ACS, Wiley, and Springer-Nature. Prof. Nguyen-Tri served also as scientific committee for several international conferences and regular member of American Chemical Society (ACS).

Payman Ghassemi obtained his Master's degree in Chemical Engineering in 2011 from UTM, Malaysia. He worked then as a research assistant at DTU Conversion Energy, Denmark. His research interests are functional polymers, nanomaterials, energy and separation technology. From 2020, he is a PhD candidate at the University of Quebec in Trois-Rivieres (UQTR), under the supervision of Prof. P. Nguyen-Tri. His thesis topic is related to the crystallization and the nanoscale characterization of miscible blends of several biodegradable and crystallizable polymers.

Pascal Carrière

Pascal Carriere is an associate Professor at University of Toulon at MAPIEM Laboratory (Materials Polymers, Interface and Marine Environnement) since 2002. He received his chemistry engineer degree from the Chemistry, Physics and Electronic Engineering School of Lyon (ICPI-CPE-Lyon). Then he did his thesis at the Institute of Chemistry of Surface and Interface in Mulhouse on conformational study of stereoregular PMMA and PMMA-PEO mixtures at silica-solvant interface and rheological behavior of this dispersion. He received his PhD degree in 2000 from the University of Haute-Alsace, France. Subsequently, he joined University of Toulon as an assistant professor and he headed the chemistry and materials department from 2003 to 2010 before being Vice-President of the University of Toulon, France from 2011 to 2015. His main research interests are polymers at interfaces, confinement studies, ultra-thin films as model of composites materials, smart interfaces and coatings for composite materials durability improvement, nanoscale characterizations of polymeric materials.

Aymen Amine Assadi

Aymen Amine Assadi is an associate professor at Institut des Sciences Chimiques de Rennes (ISCR) - UMR CNRS 6226, Université de Rennes, France. ASSADI Aymen (35 years old) has completed his PhD from Chemistry Engineer School ENSCR in Rennes, France. He joined ENSCR as associate professor in 2014.He obtained recently (June 2019) his Thesis Director Enabling Degree “HDR” (Reactor Design for Advanced Oxidation Processes – University of Rennes 1) in Process Engineering. His field of expertise concerns environmental engineering and especially the study of physical and chemical treatments in relation with traces compounds. His research focuses mainly on processes involving plasma and photocatalysis oxidation of micropollution and / or processes involving a transfer to a solid phase. With an h-index of 19, he published more than 65 Q1 ranking publications, 2 patents. He is Editor to Elsevier Book on “air remediation” and has two book-chapters and presented numerous communications at international meetings (more than 70). He is associate editor (Springer journals), guest editor and regular reviewer for many international peer reviewed journals.

Dinh Duc Nguyen

Peer-reviewed version available at Polymers 2020, 12, 1142; doi:10.3390/polym12051142

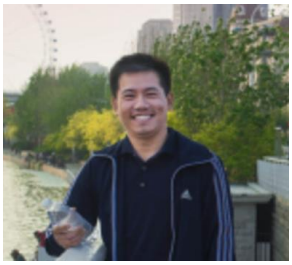

Nguyen Dinh Duc is now an assistant Professor at Department of Environmental Energy System Engineering, Kyonggi University, Seoul, South Korea. His current research interests focus on nanoscale characterization of materials; the anaerobic digestion of organic waste for the generation of renewable energy; the hybrid biological process for wastewater treatment, and preparation/synthesis of novel nanoparticles, composite materials and biochars for applications in the environmental remediation and chemical industry. He is also conducting research and development to commercial design products based research finding, for some leading environmental companies and organizations. Dr. Nguyen Dinh Duc is author and co-author of over 100 peer-reviewed journals.

References

1. Campion, A., Infrared and Raman Spectroscopy of Biological Materials. Practical Spectroscopy Series. Volume 24 Edited by Hans-Ulrich Gremlich (Novartis Pharma AG, Basel, Switzerland) and Bing Yan (ChemRx Advanced Technologies, Inc., South San Francisco, California). Marcel Dekker: New York and Basel. 2001. xii+ 582 pp. $195.00. ISBN 0-8247-0409-6. ACS Publications: 2001.

2. Koenig, J. L.; Wang, S.-Q.; Bhargava, R., Peer reviewed: FTIR images. ACS Publications: 2001.

3. Popescu, M.-C.; Filip, D.; Vasile, C.; Cruz, C.; Rueff, J.; Marcos, M.; Serrano, J.; Singurel, G., Characterization by Fourier transform infrared spectroscopy (FT-IR) and 2D IR correlation spectroscopy of PAMAM dendrimer. *The Journal of Physical Chemistry B* **2006,** *110* (29), 14198-14211.

4. Smith, P. A. M., Infrared microspectroscopy mapping studies of packaging materials: experiment design and data profiling considerations. *Vibrational Spectroscopy* **2000,** *24* (1), 47-62.

5. Tannenbaum, R.; Zubris, M.; David, K.; Ciprari, D.; Jacob, K.; Jasiuk, I.; Dan, N., FTIR characterization of the reactive interface of cobalt oxide nanoparticles embedded in polymeric matrices. *The Journal of Physical Chemistry B* **2006,** *110* (5), 2227-2232.

6. Kumar, T. S., Physical and Chemical Characterization of Biomaterials. In *Characterization of Biomaterials*, Elsevier: 2013; pp 11-47.

7. Ho, T. T.; Bremmell, K. E.; Krasowska, M.; MacWilliams, S. V.; Richard, C. l. J.; Stringer, D. N.; Beattie, D. A., In situ ATR FTIR spectroscopic study of the formation and hydration of a fucoidan/chitosan polyelectrolyte multilayer. *Langmuir* **2015,** *31* (41), 11249-11259.

8. Tejedor-Tejedor, M. I.; Paredes, L.; Anderson, M. A., Evaluation of ATR− FTIR spectroscopy as an "in situ" tool for following the hydrolysis and condensation of alkoxysilanes under rich H2O conditions. *Chemistry of materials* **1998,** *10* (11), 3410-3421.

9. Roy, S.; Perez-Guaita, D.; Andrew, D. W.; Richards, J. S.; McNaughton, D.; Heraud, P.; Wood, B. R., Simultaneous ATR-FTIR based determination of malaria parasitemia, glucose and urea in whole blood dried onto a glass slide. *Analytical chemistry* **2017,** *89* (10), 5238-5245.

10. Schuttlefield, J. D.; Grassian, V. H., ATR–FTIR spectroscopy in the undergraduate chemistry laboratory. Part I: fundamentals and examples. *Journal of chemical education* **2008,** *85* (2), 279.

11. Ami, D.; Mereghetti, P.; Foli, A.; Tasaki, M.; Milani, P.; Nuvolone, M.; Palladini, G.; Merlini, G.; Lavatelli, F.; Natalello, A., ATR-FTIR spectroscopy supported by multivariate analysis for the characterization of adipose tissue aspirates from patients affected by systemic amyloidosis. *Analytical chemistry* **2019,** *91* (4), 2894-2900.

12. Maver, U.; Maver, T.; Peršin, Z.; Mozetič, M.; Vesel, A.; Gaberšček, M.; Stana-Kleinschek, K., Polymer characterization with the atomic force microscope. *Polymer Science* **2013,** *4*.

13. Magonov, S., Atomic force microscopy in analysis of polymers. *Encyclopedia of Analytical Chemistry: Applications, Theory and Instrumentation* **2006**.

14. Vahabi, S.; Salman, B. N.; Javanmard, A., Atomic force microscopy application in biological research: a review study. *Iranian journal of medical sciences* **2013,** *38* (2), 76.

15. Last, J. A.; Russell, P.; Nealey, P. F.; Murphy, C. J., The applications of atomic force microscopy to vision science. *Investigative ophthalmology & visual science* **2010,** *51* (12), 6083-6094.

16. Stocker, W.; Schumacher, M.; Graff, S.; Thierry, A.; Wittmann, J.-C.; Lotz, B., Epitaxial crystallization and AFM investigation of a frustrated polymer structure: isotactic poly (propylene), β phase. *Macromolecules* **1998,** *31* (3), 807-814.

17. Hobbs, J.; Miles, M., Direct observation of polyethylene shish-kebab crystallization using in-situ atomic force microscopy. *Macromolecules* **2001,** *34* (3), 353-355.
18. Hobbs, J.; Humphris, A.; Miles, M., In-situ atomic force microscopy of polyethylene crystallization. 1. crystallization from an oriented backbone. *Macromolecules* **2001,** *34* (16), 5508-5519.
19. Ono, Y.; Kumaki, J., In situ real-time observation of polymer folded-chain crystallization by atomic force microscopy at the molecular level. *Macromolecules* **2018,** *51* (19), 7629-7636.
20. Schulz, M.; Seidlitz, A.; Kurz, R.; Bärenwald, R.; Petzold, A.; Saalwächter, K.; Thurn-Albrecht, T., The Underestimated Effect of Intracrystalline Chain Dynamics on the Morphology and Stability of Semicrystalline Polymers. *Macromolecules* **2018,** *51* (21), 8377-8385.
21. Sun, H.; Yu, D. M.; Shi, S.; Yuan, Q.; Fujinami, S.; Sun, X.; Wang, D.; Russell, T. P., Configurationally Constrained Crystallization of Brush Polymers with Poly (ethylene oxide) Side Chains. *Macromolecules* **2019,** *52* (2), 592-600.
22. Boissé, S. p.; Kryuchkov, M. A.; Tien, N.-D.; Bazuin, C. G. r.; Prud'homme, R. E., PLLA Crystallization in Linear AB and BAB Copolymers of l-Lactide and 2-Dimethylaminoethyl Methacrylate. *Macromolecules* **2016,** *49* (18), 6973-6986.
23. Roland, S. b.; Gamys, C. G.; Grosrenaud, J.; Boissé, S. p.; Pellerin, C.; Prud'homme, R. E.; Bazuin, C. G., Solvent Influence on thickness, composition, and morphology variation with dip-coating rate in supramolecular PS-b-P4VP thin films. *Macromolecules* **2015,** *48* (14), 4823-4834.
24. Mareau, V. H.; Prud'Homme, R. E., In-situ hot stage atomic force microscopy study of poly (ε-caprolactone) crystal growth in ultrathin films. *Macromolecules* **2005,** *38* (2), 398-408.
25. Maillard, D.; Prud'Homme, R. E., Crystallization of ultrathin films of polylactides: from chain chirality to lamella curvature and twisting. *Macromolecules* **2008,** *41* (5), 1705-1712.
26. Vielmuth, F.; Spindler, V.; Waschke, J., Atomic force microscopy provides new mechanistic insights into the pathogenesis of pemphigus. *Frontiers in Immunology* **2018,** *9*, 485.
27. Baker, A.; Helbert, W.; Sugiyama, J.; Miles, M., New insight into cellulose structure by atomic force microscopy shows the Iα crystal phase at near-atomic resolution. *Biophysical Journal* **2000,** *79* (2), 1139-1145.
28. Dufrêne, Y. F., Atomic force microscopy in microbiology: new structural and functional insights into the microbial cell surface. *MBio* **2014,** *5* (4), e01363-14.
29. Maver, U.; Velnar, T.; Gaberšček, M.; Planinšek, O.; Finšgar, M., Recent progressive use of atomic force microscopy in biomedical applications. *TrAC Trends in Analytical Chemistry* **2016,** *80*, 96-111.
30. Edwardson, J. M.; Henderson, R. M., Atomic force microscopy and drug discovery. *Drug discovery today* **2004,** *9* (2), 64-71.
31. Senapati, S.; Lindsay, S., Recent progress in molecular recognition imaging using atomic force microscopy. *Accounts of chemical research* **2016,** *49* (3), 503-510.
32. Soon, R. L.; Nation, R. L.; Hartley, P. G.; Larson, I.; Li, J., Atomic force microscopy investigation of the morphology and topography of colistin-heteroresistant Acinetobacter baumannii strains as a function of growth phase and in response to colistin treatment. *Antimicrobial agents and chemotherapy* **2009,** *53* (12), 4979-4986.
33. Shan, Y.; Wang, H., The structure and function of cell membranes examined by atomic force microscopy and single-molecule force spectroscopy. *Chemical Society Reviews* **2015,** *44* (11), 3617-3638.

34. Marrese, M.; Guarino, V.; Ambrosio, L., Atomic force microscopy: a powerful tool to address scaffold design in tissue engineering. *Journal of functional biomaterials* **2017,** *8* (1), 7.

35. Liu, Y.; Collins, L.; Proksch, R.; Kim, S.; Watson, B. R.; Doughty, B.; Calhoun, T. R.; Ahmadi, M.; Ievlev, A. V.; Jesse, S., Chemical nature of ferroelastic twin domains in CH 3 NH 3 PbI 3 perovskite. *Nature materials* **2018,** *17* (11), 1013-1019.

36. Yang, J.; Hatcherian, J.; Hackley, P. C.; Pomerantz, A. E., Nanoscale geochemical and geomechanical characterization of organic matter in shale. *Nature communications* **2017,** *8* (1), 1-9.

37. Jin, M.; Lu, F.; Belkin, M. A., High-sensitivity infrared vibrational nanospectroscopy in water. *Light: Science & Applications* **2017,** *6* (7), e17096-e17096.

38. Hassenkam, T.; Andersson, M.; Dalby, K.; Mackenzie, D.; Rosing, M., Elements of Eoarchean life trapped in mineral inclusions. *Nature* **2017,** *548* (7665), 78-81.

39. Qin, N.; Zhang, S.; Jiang, J.; Corder, S. G.; Qian, Z.; Zhou, Z.; Lee, W.; Liu, K.; Wang, X.; Li, X., Nanoscale probing of electron-regulated structural transitions in silk proteins by near-field IR imaging and nano-spectroscopy. *Nature communications* **2016,** *7* (1), 1-8.

40. Khanikaev, A. B.; Arju, N.; Fan, Z.; Purtseladze, D.; Lu, F.; Lee, J.; Sarriugarte, P.; Schnell, M.; Hillenbrand, R.; Belkin, M., Experimental demonstration of the microscopic origin of circular dichroism in two-dimensional metamaterials. *Nature communications* **2016,** *7* (1), 1-8.

41. O'callahan, B. T.; Jones, A. C.; Park, J. H.; Cobden, D. H.; Atkin, J. M.; Raschke, M. B., Inhomogeneity of the ultrafast insulator-to-metal transition dynamics of VO 2. *Nature communications* **2015,** *6* (1), 1-8.

42. Ruggeri, F.; Longo, G.; Faggiano, S.; Lipiec, E.; Pastore, A.; Dietler, G., Infrared nanospectroscopy characterization of oligomeric and fibrillar aggregates during amyloid formation. *Nature communications* **2015,** *6* (1), 1-9.

43. Ghosh, S.; Kouamé, N. A.; Ramos, L.; Remita, S.; Dazzi, A.; Deniset-Besseau, A.; Beaunier, P.; Goubard, F.; Aubert, P.-H.; Remita, H., Conducting polymer nanostructures for photocatalysis under visible light. *Nature materials* **2015,** *14* (5), 505-511.

44. Lu, F.; Jin, M.; Belkin, M. A., Tip-enhanced infrared nanospectroscopy via molecular expansion force detection. *Nature photonics* **2014,** *8* (4), 307.

45. Gao, L.; Zhao, H.; Li, T.; Huo, P.; Chen, D.; Liu, B., Atomic force microscopy based tip-enhanced Raman spectroscopy in biology. *International journal of molecular sciences* **2018,** *19* (4), 1193.

46. Huang, T.-X.; Li, C.-W.; Yang, L.-K.; Zhu, J.-F.; Yao, X.; Liu, C.; Lin, K.-Q.; Zeng, Z.-C.; Wu, S.-S.; Wang, X., Rational fabrication of silver-coated AFM TERS tips with a high enhancement and long lifetime. *Nanoscale* **2018,** *10* (9), 4398-4405.

47. Hegenbarth, R.; Steinmann, A.; Mastel, S.; Amarie, S.; Huber, A.; Hillenbrand, R.; Sarkisov, S. Y.; Giessen, H., High-power femtosecond mid-IR sources for s-SNOM applications. *Journal of optics* **2014,** *16* (9), 094003.

48. Hoffmann, W. D.; Kertesz, V.; Srijanto, B. R.; Van Berkel, G. J., Atomic Force Microscopy Thermally-Assisted Microsampling with Atmospheric Pressure Temperature Ramped Thermal Desorption/Ionization-Mass Spectrometry Analysis. *Analytical chemistry* **2017,** *89* (5), 3036-3042.

49. Owens, S. C.; Berenbeim, J. A.; Patterson, C. S.; Dillon, E. P.; de Vries, M., Sub-micron proximal probe thermal desorption and laser mass spectrometry on painting cross-sections. *Analytical Methods* **2014,** *6* (22), 8940-8945.

50. Goh, C. F.; Moffat, J. G.; Craig, D. Q.; Hadgraft, J.; Lane, M. E., Nano-thermal imaging of the stratum corneum and its potential use for understanding of the mechanism of skin penetration enhancer. *Thermochimica Acta* **2017,** *655*, 278-283.

51. Yavari, M.; Maruf, S.; Ding, Y.; Lin, H., Physical aging of glassy perfluoropolymers in thin film composite membranes. Part II. Glass transition temperature and the free volume model. *Journal of membrane science* **2017,** *525*, 399-408.

52. Dazzi, A.; Prazeres, R.; Glotin, F.; Ortega, J., Local infrared microspectroscopy with subwavelength spatial resolution with an atomic force microscope tip used as a photothermal sensor. *Optics letters* **2005,** *30* (18), 2388-2390.

53. Mathurin, J.; Pancani, E.; Deniset-Besseau, A.; Kjoller, K.; Prater, C. B.; Gref, R.; Dazzi, A., How to unravel the chemical structure and component localization of individual drug-loaded polymeric nanoparticles by using tapping AFM-IR. *Analyst* **2018,** *143* (24), 5940-5949.

54. Pancani, E.; Mathurin, J.; Bilent, S.; Bernet-Camard, M. F.; Dazzi, A.; Deniset-Besseau, A.; Gref, R., High-Resolution Label-Free Detection of Biocompatible Polymeric Nanoparticles in Cells. *Particle & Particle Systems Characterization* **2018,** *35* (3), 1700457.

55. Hinrichs, K.; Shaykhutdinov, T., Polarization-Dependent Atomic Force Microscopy–Infrared Spectroscopy (AFM-IR): Infrared Nanopolarimetric Analysis of Structure and Anisotropy of Thin Films and Surfaces. *Applied spectroscopy* **2018,** *72* (6), 817-832.

56. Murdick, R. A.; Morrison, W.; Nowak, D.; Albrecht, T. R.; Jahng, J.; Park, S., Photoinduced force microscopy: A technique for hyperspectral nanochemical mapping. *Japanese Journal of Applied Physics* **2017,** *56* (8S1), 08LA04.

57. Mousoulis, C.; Maleki, T.; Ziaie, B.; Neu, C. P., Atomic force microscopy-coupled microcoils for cellular-scale nuclear magnetic resonance spectroscopy. *Applied physics letters* **2013,** *102* (14), 143702.

58. Lherbette, M.; Dos Santos, Á.; Hari-Gupta, Y.; Fili, N.; Toseland, C. P.; Schaap, I. A., Atomic Force Microscopy micro-rheology reveals large structural inhomogeneities in single cell-nuclei. *Scientific reports* **2017,** *7* (1), 1-13.

59. Nalam, P. C.; Gosvami, N. N.; Caporizzo, M. A.; Composto, R. J.; Carpick, R. W., Nano-rheology of hydrogels using direct drive force modulation atomic force microscopy. *Soft Matter* **2015,** *11* (41), 8165-8178.

60. Dazzi, A.; Prater, C. B., AFM-IR: technology and applications in nanoscale infrared spectroscopy and chemical imaging. *Chemical reviews* **2017,** *117* (7), 5146-5173.

61. Centrone, A., Infrared imaging and spectroscopy beyond the diffraction limit. **2015**.

62. Fu, W.; Zhang, W., Hybrid AFM for nanoscale physicochemical characterization: recent development and emerging applications. *small* **2017,** *13* (11), 1603525.

63. Xiao, L.; Schultz, Z. D., Spectroscopic imaging at the nanoscale: technologies and recent applications. *Analytical chemistry* **2018,** *90* (1), 440-458.

64. Gong, L.; Chase, D. B.; Noda, I.; Liu, J.; Martin, D. C.; Ni, C.; Rabolt, J. F., Discovery of β-form crystal structure in electrospun poly [(R)-3-hydroxybutyrate-co-(R)-3-hydroxyhexanoate](PHBHx) nanofibers: From fiber mats to single fibers. *Macromolecules* **2015,** *48* (17), 6197-6205.

65. Tang, F.; Bao, P.; Su, Z., Analysis of nanodomain composition in high-impact polypropylene by atomic force microscopy-infrared. *Analytical chemistry* **2016,** *88* (9), 4926-4930.

66. Purohit, H. S.; Taylor, L. S., Miscibility of itraconazole–hydroxypropyl methylcellulose blends: Insights with high resolution analytical methodologies. *Molecular pharmaceutics* **2015,** *12* (12), 4542-4553.

67. Van Eerdenbrugh, B.; Lo, M.; Kjoller, K.; Marcott, C.; Taylor, L. S., Nanoscale mid-infrared evaluation of the miscibility behavior of blends of dextran or maltodextrin with poly (vinylpyrrolidone). *Molecular pharmaceutics* **2012,** *9* (5), 1459-1469.

68. Ma, X.; Zhou, X.; Yu, A.; Zhao, W.; Zhang, W.; Zhang, S.; Wei, L.; Cook, D. J.; Roy, A., Functionalized metal-organic framework nanocomposites for dispersive solid phase extraction and enantioselective capture of chiral drug intermediates. *Journal of Chromatography A* **2018,** *1537*, 1-9.

69. Mikhalchan, A.; Banas, A. M.; Banas, K.; Borkowska, A. M.; Nowakowski, M.; Breese, M. B.; Kwiatek, W. M.; Paluszkiewicz, C.; Tay, T. E., Revealing chemical heterogeneity of CNT fiber nanocomposites via nanoscale chemical imaging. *Chemistry of Materials* **2018,** *30* (6), 1856-1864.

70. Ali, A.; Morrow, P.; Henda, R.; Fagerberg, R., Deposition of cobalt doped zinc oxide thin film nano-composites via pulsed electron beam ablation. *MRS Advances* **2016,** *1* (6), 433-439.

71. Van Assche, G.; Van Mele, B., Interphase formation in model composites studied by micro-thermal analysis. *Polymer* **2002,** *43* (17), 4605-4610.

72. Kelchtermans, M.; Lo, M.; Dillon, E.; Kjoller, K.; Marcott, C., Characterization of a polyethylene–polyamide multilayer film using nanoscale infrared spectroscopy and imaging. *Vibrational Spectroscopy* **2016,** *82*, 10-15.

73. Wang, H.; Wang, C.-T.; Xu, F.; Yang, J.; Liu, J.; Cai, W.; Zhu, G., Resistive switching and nanoscale chemical mapping of phase separation in PVDF/PMMA/F8T2 ternary thin films. *Polymer* **2018,** *153*, 498-506.

74. Perez-Guaita, D.; Kochan, K.; Batty, M.; Doerig, C.; Garcia-Bustos, J.; Espinoza, S.; McNaughton, D.; Heraud, P.; Wood, B. R., Multispectral atomic force microscopy-infrared nano-imaging of malaria infected red blood cells. *Analytical chemistry* **2018,** *90* (5), 3140-3148.

75. Shaykhutdinov, T.; Pop, S. D.; Furchner, A.; Hinrichs, K., Supramolecular orientation in anisotropic assemblies by infrared nanopolarimetry. *ACS Macro Letters* **2017,** *6* (6), 598-602.

76. Waeytens, J.; Doneux, T.; Napolitano, S., Evaluating Mechanical Properties of Polymers at the Nanoscale Level via Atomic Force Microscopy–Infrared Spectroscopy. *ACS Applied Polymer Materials* **2018,** *1* (1), 3-7.

77. Crist, B.; Schultz, J. M., Atomic Force Microscopy Studies of Polymer Crystals: Nucleation, Growth, Annealing, and Melting. In *Encyclopedia of Polymers and Composites*, Palsule, S., Ed. Springer Berlin Heidelberg: Berlin, Heidelberg, 2021; pp 1-25.

78. Zhu, D.; Shou, X.; Liu, Y.; Chen, E.; Cheng, S. Z., AFM-tip-induced crystallization of poly (ethylene oxide) melt droplets. *Frontiers of Chemistry in China* **2007,** *2* (2), 174-177.

79. Magonov, S. N.; Reneker, D. H., Characterization of polymer surfaces with atomic force microscopy. *Annual Review of Materials Science* **1997,** *27* (1), 175-222.

80. Klinov, D.; Magonov, S., True molecular resolution in tapping-mode atomic force microscopy with high-resolution probes. *Applied physics letters* **2004,** *84* (14), 2697-2699.

81. Pearce, R.; Vancso, G. J., Real-time imaging of melting and crystallization in poly (ethylene oxide) by atomic force microscopy. *Polymer* **1998,** *39* (5), 1237-1242.

82. Pearce, R.; Vancso, G. J., Imaging of melting and crystallization of poly (ethylene oxide) in real-time by hot-stage atomic force microscopy. *Macromolecules* **1997,** *30* (19), 5843-5848.
83. McMaster, T.; Hobbs, J.; Barham, P.; Miles, M., AFM study of in situ real time polymer crystallization and spherulite structure. *Probe Microscopy* **1997,** *1* (1), 43-56.
84. Hobbs, J.; McMaster, T.; Miles, M.; Barham, P., Direct observations of the growth of spherulites of poly (hydroxybutyrate-co-valerate) using atomic force microscopy. *Polymer* **1998,** *39* (12), 2437-2446.
85. Sitterberg, J.; Özcetin, A.; Ehrhardt, C.; Bakowsky, U., Utilising atomic force microscopy for the characterisation of nanoscale drug delivery systems. *European Journal of Pharmaceutics and Biopharmaceutics* **2010,** *74* (1), 2-13.
86. Meyer, E., Heinzelmann in Scanning Tunneling Microscopy II. Heidelberg, Springer: 1992.
87. Hobbs, J. K.; Farrance, O. E.; Kailas, L., How atomic force microscopy has contributed to our understanding of polymer crystallization. *Polymer* **2009,** *50* (18), 4281-4292.
88. Jagtap, R.; Ambre, A., Overview literature on atomic force microscopy (AFM): Basics and its important applications for polymer characterization. **2006**.
89. Braga, P. C.; Ricci, D., *Atomic force microscopy: biomedical methods and applications*. Springer Science & Business Media: 2004; Vol. 242.
90. Eaton , P., AFM: Beginner's Guide. **2009**.
91. Schmitz, I.; Schreiner, M.; Friedbacher, G.; Grasserbauer, M., Phase imaging as an extension to tapping mode AFM for the identification of material properties on humidity-sensitive surfaces. *Applied surface science* **1997,** *115* (2), 190-198.
92. Winkler, R.; Spatz, J.; Sheiko, S.; Möller, M.; Reineker, P.; Marti, O., Imaging material properties by resonant tapping-force microscopy: a model investigation. *Physical Review B* **1996,** *54* (12), 8908.
93. Lin, W.-C.; Blanchette, C. D.; Ratto, T. V.; Longo, M. L., Lipid asymmetry in DLPC/DSPC-supported lipid bilayers: a combined AFM and fluorescence microscopy study. *Biophysical journal* **2006,** *90* (1), 228-237.
94. Simon, M.; Wittmar, M.; Bakowsky, U.; Kissel, T., Self-assembling nanocomplexes from insulin and water-soluble branched polyesters, poly [(vinyl-3-(diethylamino)-propylcarbamate-co-(vinyl acetate)-co-(vinyl alcohol)]-graft-poly (l-lactic acid): a novel carrier for transmucosal delivery of peptides. *Bioconjugate chemistry* **2004,** *15* (4), 841-849.
95. Butt, H.-J.; Cappella, B.; Kappl, M., Force measurements with the atomic force microscope: Technique, interpretation and applications. *Surface science reports* **2005,** *59* (1-6), 1-152.
96. Wong, J.; Chilkoti, A.; Moy, V. T., Direct force measurements of the streptavidin–biotin interaction. *Biomolecular engineering* **1999,** *16* (1-4), 45-55.
97. Radmacher, M.; Cleveland, J. P.; Fritz, M.; Hansma, H. G.; Hansma, P. K., Mapping interaction forces with the atomic force microscope. *Biophysical journal* **1994,** *66* (6), 2159-2165.
98. Quist, A. P.; Bergman, A. A.; Reimann, C. T.; Oscarsson, S. O.; Sundqvist, B., Imaging of single antigens, antibodies, and specific immunocomplex formation by scanning force microscopy. *Scanning microscopy* **1995,** *9* (2), 395-400.
99. Florin, E.-L.; Moy, V. T.; Gaub, H. E., Adhesion forces between individual ligand-receptor pairs. *Science* **1994,** *264* (5157), 415-417.

100. Chen, A.; Moy, V. T., Cross-linking of cell surface receptors enhances cooperativity of molecular adhesion. *Biophysical Journal* **2000,** *78* (6), 2814-2820.
101. Rimondini, L.; Bianchi, C. L.; Vernè, E., *Surface tailoring of inorganic materials for biomedical applications*. Bentham Science Publishers: 2012.
102. Villarrubia, J. S., Morphological estimation of tip geometry for scanned probe microscopy. *Surface science* **1994,** *321* (3), 287-300.
103. Keller, D. J.; Chih-Chung, C., Imaging steep, high structures by scanning force microscopy with electron beam deposited tips. *Surface Science* **1992,** *268* (1-3), 333-339.
104. Micic, M.; Chen, A.; Leblanc, R. M.; Moy, V. T., Scanning electron microscopy studies of protein-functionalized atomic force microscopy cantilever tips. *Scanning* **1999,** *21* (6), 394-397.
105. Baden, N.; Yasuda, M.; Yoshida, A.; Muraki, N. In *New method for chemical characterization of polymer materials in industrial devices: AFM-IR with FIB sample preparation*, 2015 IEEE 22nd International Symposium on the Physical and Failure Analysis of Integrated Circuits, IEEE: 2015; pp 496-499.
106. Ni, G.; Wang, L.; Goldflam, M.; Wagner, M.; Fei, Z.; McLeod, A.; Liu, M.; Keilmann, F.; Özyilmaz, B.; Neto, A. C., Ultrafast optical switching of infrared plasmon polaritons in high-mobility graphene. *Nature Photonics* **2016,** *10* (4), 244-247.
107. Dazzi, A.; Prater, C. B.; Hu, Q.; Chase, D. B.; Rabolt, J. F.; Marcott, C., AFM–IR: combining atomic force microscopy and infrared spectroscopy for nanoscale chemical characterization. *Applied spectroscopy* **2012,** *66* (12), 1365-1384.
108. Lu, F.; Belkin, M. A., Infrared absorption nano-spectroscopy using sample photoexpansion induced by tunable quantum cascade lasers. *Optics express* **2011,** *19* (21), 19942-19947.
109. Wieland, K.; Ramer, G.; Weiss, V. U.; Allmaier, G.; Lendl, B.; Centrone, A., Nanoscale chemical imaging of individual chemotherapeutic cytarabine-loaded liposomal nanocarriers. *Nano research* **2019,** *12* (1), 197-203.
110. Tuteja, M.; Kang, M.; Leal, C.; Centrone, A., Nanoscale partitioning of paclitaxel in hybrid lipid–polymer membranes. *Analyst* **2018,** *143* (16), 3808-3813.
111. Cuberes, M. T.; Assender, H.; Briggs, G. A. D.; Kolosov, O., Heterodyne force microscopy of PMMA/rubber nanocomposites: nanomapping of viscoelastic response at ultrasonic frequencies. *Journal of Physics D: Applied Physics* **2000,** *33* (19), 2347.
112. Cuberes, M. T., Intermittent-contact heterodyne force microscopy. *Journal of Nanomaterials* **2009,** *2009*.
113. Verbiest, G.; Oosterkamp, T.; Rost, M., Subsurface-AFM: sensitivity to the heterodyne signal. *Nanotechnology* **2013,** *24* (36), 365701.
114. Harding, L.; King, W. P.; Dai, X.; Craig, D. Q.; Reading, M., Nanoscale characterisation and imaging of partially amorphous materials using local thermomechanical analysis and heated tip AFM. *Pharmaceutical research* **2007,** *24* (11), 2048-2054.
115. Mueller, T., Quantitative nanoscale characterization. *Materials Today* **2009,** *12* (9), 40-43.
116. Bozec, L.; Odlyha, M., Thermal denaturation studies of collagen by microthermal analysis and atomic force microscopy. *Biophysical journal* **2011,** *101* (1), 228-236.
117. Nguyen-Tri, P.; Ouellet-Plamondon, C., Nanoscale characterization and interfacial crystallization of natural hollow milkweed fibers reinforced PCL/PVC. **2018**.

118. Nguyen-Tri, P.; Nguyen, V. T.; Nguyen, T. A., Biological activity and nanostructuration of Fe3O4-Ag/high density polyethylene nanocomposites. *Journal of Composites Science* **2019,** *3* (2), 34.
119. Prater, C.; Kjoller, K.; Cook, D.; Shetty, R.; Meyers, G.; Reinhardt, C.; Felts, J.; King, W.; Vodopyanov, K.; Dazzi, A., Nanoscale infrared spectroscopy of materials by atomic force microscopy. *Microscopy and Analysis-UK* **2010,** (138), 5.
120. Ye, J.; Midorikawa, H.; Awatani, T.; Marcott, C.; Lo, M.; Kjoller, K.; Shetty, R., Nanoscale infrared spectroscopy and AFM imaging of a polycarbonate/acrylonitrile-styrene/butadiene blend. *Microsc. Anal* **2012,** *26*, 24-27.
121. Felts, J. R.; Kjoller, K.; Lo, M.; Prater, C. B.; King, W. P., Nanometer-scale infrared spectroscopy of heterogeneous polymer nanostructures fabricated by tip-based nanofabrication. *ACS nano* **2012,** *6* (9), 8015-8021.
122. Felts, J. R.; Somnath, S.; Ewoldt, R. H.; King, W. P., Nanometer-scale flow of molten polyethylene from a heated atomic force microscope tip. *Nanotechnology* **2012,** *23* (21), 215301.
123. Van Eerdenbrugh, B.; Lo, M.; Kjoller, K.; Marcott, C.; Taylor, L. S., Nanoscale mid-infrared imaging of phase separation in a drug–polymer blend. *Journal of pharmaceutical sciences* **2012,** *101* (6), 2066-2073.
124. Marcott, C.; Awatani, T.; Ye, J.; Gerrard, D.; Lod, M.; Kjollerd, K., Review of nanoscale infrared spectroscopy applications to energy related materials. *Spectroscopy Europe26* **2014**, 19-23.
125. Tipduangta, P.; Belton, P.; Fabian, L.; Wang, L. Y.; Tang, H.; Eddleston, M.; Qi, S., Electrospun polymer blend nanofibers for tunable drug delivery: the role of transformative phase separation on controlling the release rate. *Molecular pharmaceutics* **2016,** *13* (1), 25-39.
126. Li, N.; Taylor, L. S., Nanoscale infrared, thermal, and mechanical characterization of telaprevir–polymer miscibility in amorphous solid dispersions prepared by solvent evaporation. *Molecular pharmaceutics* **2016,** *13* (3), 1123-1136.
127. Nguyen Tri, P.; Prud'homme, R. E., Crystallization and segregation behavior at the submicrometer scale of PCL/PEG blends. *Macromolecules* **2018,** *51* (18), 7266-7273.
128. Tang, F.; Bao, P.; Roy, A.; Wang, Y.; Su, Z., In-situ spectroscopic and thermal analyses of phase domains in high-impact polypropylene. *Polymer* **2018,** *142*, 155-163.
129. Keddie, J. L.; Jones, R. A.; Cory, R. A., Size-dependent depression of the glass transition temperature in polymer films. *EPL (Europhysics Letters)* **1994,** *27* (1), 59.
130. Tsui, O.; Russell, T.; Hawker, C., Effect of interfacial interactions on the glass transition of polymer thin films. *Macromolecules* **2001,** *34* (16), 5535-5539.
131. Riedel, C.; Sweeney, R.; Israeloff, N. E.; Arinero, R.; Schwartz, G. A.; Alegría, A.; Tordjeman, P.; Colmenero, J., Imaging dielectric relaxation in nanostructured polymers by frequency modulation electrostatic force microscopy. *Applied Physics Letters* **2010,** *96* (21), 213110.
132. Yang, Z.; Fujii, Y.; Lee, F. K.; Lam, C.-H.; Tsui, O. K., Glass transition dynamics and surface layer mobility in unentangled polystyrene films. *Science* **2010,** *328* (5986), 1676-1679.
133. Garcia, R.; Perez, R., SURF SCI REP. *Surf Sci Rep* **2002,** *47*, 197-301.
134. Fasolka, M. J.; Mayes, A. M.; Magonov, S. N., Thermal enhancement of AFM phase contrast for imaging diblock copolymer thin film morphology. *Ultramicroscopy* **2001,** *90* (1), 21-31.
135. Reiter, G.; Sommer, J.-U., *Polymer Crystallization: Obervations, Concepts and Interpretations*. Springer Science & Business Media: 2003; Vol. 606.

136. Kikkawa, Y.; Abe, H.; Fujita, M.; Iwata, T.; Inoue, Y.; Doi, Y., Crystal growth in poly (L-lactide) thin film revealed by in situ atomic force microscopy. *Macromolecular Chemistry and Physics* **2003,** *204* (15), 1822-1831.

137. Zhou, J.-J.; Liu, J.-G.; Yan, S.-K.; Dong, J.-Y.; Li, L.; Chan, C.-M.; Schultz, J. M., Atomic force microscopy study of the lamellar growth of isotactic polypropylene. *Polymer* **2005,** *46* (12), 4077-4087.

138. Humphris, A.; Miles, M.; Hobbs, J., A mechanical microscope: High-speed atomic force microscopy. *Applied physics letters* **2005,** *86* (3), 034106.

139. Tognana, S. A.; Salgueiro, W. A.; Silva, L., A SAXS study of PHB/DGEBA blends crystallized at different temperatures. *Procedia Materials Science* **2015,** *8*.

140. Reddy, K. R.; Ogawa, S.; Sato, H.; Takahashi, I.; Ozaki, Y., Evolution of intermediate and highly ordered crystalline states under spatial confinement in poly (3-hydroxybutyrate) ultrathin films. *Macromolecules* **2016,** *49* (11), 4202-4210.

141. Rosenthal, M.; Burghammer, M.; Bar, G.; Samulski, E. T.; Ivanov, D. A., Switching chirality of hybrid left–right crystalline helicoids built of achiral polymer chains: When right to left becomes left to right. *Macromolecules* **2014,** *47* (23), 8295-8304.

142. Ivanov, D. A.; Rosenthal, M., Microstructure of banded polymer spherulites: New insights from synchrotron nanofocus X-ray scattering. In *Polymer Crystallization II*, Springer: 2016; pp 95-126.

143. Prud'homme, R. E., Crystallization and morphology of ultrathin films of homopolymers and polymer blends. *Progress in Polymer Science* **2016,** *54*, 214-231.

144. Tri, P. N.; Prud'homme, R. E., Nanoscale lamellar assembly and segregation mechanism of poly (3-hydroxybutyrate)/poly (ethylene glycol) blends. *Macromolecules* **2018,** *51* (1), 181-188.

145. Nguyen-Tri, P.; Prud'homme, R. E., Nanoscale analysis of the photodegradation of polyester fibers by AFM-IR. *Journal of Photochemistry and Photobiology A: Chemistry* **2019,** *371*, 196-204.

146. Zeb, G.; Tri, P. N.; Palacin, S.; Le, X. T., Pulse potential deposition of thick polyvinylpyridine-like film on the surface of titanium nitride. *RSC advances* **2016,** *6* (84), 80825-80829.

147. Nguyen, T. V.; Le, X. H.; Dao, P. H.; Decker, C.; Nguyen-Tri, P., Stability of acrylic polyurethane coatings under accelerated aging tests and natural outdoor exposure: The critical role of the used photo-stabilizers. *Progress in Organic Coatings* **2018,** *124*, 137-146.

148. Prater, C.; Kjoller, K.; Shetty, R., Nanoscale infrared spectroscopy. *Materials Today* **2010,** *13* (11), 56-60.

149. Marcott, C.; Lo, M.; Dillon, E.; Kjoller, K.; Prater, C., Interface analysis of composites using AFM-based nanoscale IR and mechanical spectroscopy. *Microscopy Today* **2015,** *23* (2), 38-45.

150. Xiao, L.; Deng, M.; Zeng, W.; Zhang, B.; Xu, Z.; Yi, C.; Liao, G., Novel robust superhydrophobic coating with self-cleaning properties in air and oil based on rare earth metal oxide. *Industrial & Engineering Chemistry Research* **2017,** *56* (43), 12354-12361.

151. Cao, L.; Jones, A. K.; Sikka, V. K.; Wu, J.; Gao, D., Anti-icing superhydrophobic coatings. *Langmuir* **2009,** *25* (21), 12444-12448.

152. Das, S.; Kumar, S.; Samal, S. K.; Mohanty, S.; Nayak, S. K., A review on superhydrophobic polymer nanocoatings: recent development and applications. *Industrial & Engineering Chemistry Research* **2018,** *57* (8), 2727-2745.

153. Chevallier, P.; Turgeon, S.; Sarra-Bournet, C.; Turcotte, R.; Laroche, G., Characterization of multilayer anti-fog coatings. *ACS applied materials & interfaces* **2011,** *3* (3), 750-758.
154. Chang, C.-C.; Huang, F.-H.; Chang, H.-H.; Don, T.-M.; Chen, C.-C.; Cheng, L.-P., Preparation of water-resistant antifog hard coatings on plastic substrate. *Langmuir* **2012,** *28* (49), 17193-17201.
155. Mohammadi, R.; Wassink, J.; Amirfazli, A., Effect of surfactants on wetting of super-hydrophobic surfaces. *Langmuir* **2004,** *20* (22), 9657-9662.
156. Kong, X.; Zhang, J.; Xuan, Q.; Lu, J.; Feng, J., Superhydrophobic coating for antifouling of Chinese paintings. *Langmuir* **2018,** *34* (28), 8294-8301.
157. Lu, Z.; Chen, Z.; Guo, Y.; Ju, Y.; Liu, Y.; Feng, R.; Xiong, C.; Ober, C. K.; Dong, L., Flexible hydrophobic antifouling coating with oriented nanotopography and nonleaking capsaicin. *ACS applied materials & interfaces* **2018,** *10* (11), 9718-9726.
158. Brown, P. S.; Bhushan, B., Durable, superoleophobic polymer–nanoparticle composite surfaces with re-entrant geometry via solvent-induced phase transformation. *Scientific reports* **2016,** *6*, 21048.
159. Wei, T.; Tang, Z.; Yu, Q.; Chen, H., Smart antibacterial surfaces with switchable bacteria-killing and bacteria-releasing capabilities. *ACS applied materials & interfaces* **2017,** *9* (43), 37511-37523.
160. Brown, L. V.; Davanco, M.; Sun, Z.; Kretinin, A.; Chen, Y.; Matson, J. R.; Vurgaftman, I.; Sharac, N.; Giles, A. J.; Fogler, M. M., Nanoscale mapping and spectroscopy of nonradiative hyperbolic modes in hexagonal boron nitride nanostructures. *Nano letters* **2018,** *18* (3), 1628-1636.
161. Morsch, S.; Liu, Y.; Lyon, S. B.; Gibbon, S. R., Insights into epoxy network nanostructural heterogeneity using AFM-IR. *ACS applied materials & interfaces* **2016,** *8* (1), 959-966.
162. Mayet, C.; Deniset-Besseau, A.; Prazeres, R.; Ortega, J.-M.; Dazzi, A., Analysis of bacterial polyhydroxybutyrate production by multimodal nanoimaging. *Biotechnology advances* **2013,** *31* (3), 369-374.
163. Nguyen, T. V.; Tri, P. N.; Nguyen, T. D.; El Aidani, R.; Decker, C., Accelerated degradation of water borne acrylic nanocomposites used in outdoor protective coatings. *Polymer degradation and stability* **2016,** *128*, 65-76.
164. Nguyen-Tri, P.; El Aidani, R.; Leborgne, É.; Pham, T.; Vu-Khanh, T., Chemical ageingaging of a polyester nonwoven membrane used in aerosol and drainage filter. *Polymer degradation and stability* **2014,** *101*, 71-80.
165. El Aidani, R.; Nguyen-Tri, P.; Malajati, Y.; Lara, J.; Vu-Khanh, T., Photochemical aging of an e-PTFE/NOMEX® membrane used in firefighter protective clothing. *Polymer degradation and stability* **2013,** *98* (7), 1300-1310.
166. Elias, H.-G., Chemical Aging. In *Macromolecules*, Springer: 1977; pp 843-859.
167. Morsch, S.; Lyon, S.; Greensmith, P.; Smith, S.; Gibbon, S., Mapping water uptake in organic coatings using AFM-IR. *Faraday discussions* **2015,** *180*, 527-542.
168. Morsch, S.; Lyon, S.; Gibbon, S., The degradation mechanism of an epoxy-phenolic can coating. *Progress in Organic Coatings* **2017,** *102*, 37-43.
169. Morsch, S.; Liu, Y.; Greensmith, P.; Lyon, S. B.; Gibbon, S. R., Molecularly controlled epoxy network nanostructures. *Polymer* **2017,** *108*, 146-153.
170. Morsch, S.; Van Driel, B. A.; van den Berg, K. J.; Dik, J., Investigating the photocatalytic degradation of oil paint using ATR-IR and AFM-IR. *ACS Applied Materials & Interfaces* **2017,** *9* (11), 10169-10179.

171. Morsch, S.; Bastidas, P. D.; Rowland, S. M., AFM-IR insights into the chemistry of interfacial tracking. *Journal of Materials Chemistry A* **2017,** *5* (46), 24508-24517.

172. Shiraishi, F.; Maruoka, D.; Tanoue, Y., A better UV light and TiO2-PET sheet arrangement for enhancing photocatalytic decomposition of volatile organic compounds. *Separation and Purification Technology* **2017,** *175*, 185-193.

173. Hurley, C. R.; Leggett, G. J., Quantitative investigation of the photodegradation of polyethylene terephthalate film by friction force microscopy, contact-angle goniometry, and X-ray photoelectron spectroscopy. *ACS applied materials & interfaces* **2009,** *1* (8), 1688-1697.

174. Funabashi, M.; Ninomiya, F.; Oishi, A.; Ouchi, A.; Hagihara, H.; Suda, H.; Kunioka, M., Highly accelerated aging method for poly (ethylene terephthalate) film using xenon lamp with heating system. *Journal of Polymers* **2016,** *2016*.

175. Lin, C.-C.; Krommenhoek, P. J.; Watson, S. S.; Gu, X., Depth profiling of degradation of multilayer photovoltaic backsheets after accelerated laboratory weathering: Cross-sectional Raman imaging. *Solar Energy Materials and Solar Cells* **2016,** *144*, 289-299.